

**ESTIMATION OF THE DOSE RATE OF NUCLEAR FUEL OF GHANA
RESEARCH REACTOR-1 (GHARR-1)**

A DISSERTATION SUBMITTED TO THE DEPARTMENT OF NUCLEAR
ENGINEERING, SCHOOL OF NUCLEAR AND ALLIED SCIENCES

UNIVERSITY OF GHANA, LEGON

BY

PEARL AMA ADOMAH ESSEL

10504253

IN PARTIAL FULFILLMENT OF THE REQUIREMENT FOR THE DEGREE OF
MASTER OF PHILOSOPHY IN NUCLEAR ENGINEERING

JULY, 2016

DECLARATION

I declare that apart from references of other people's work, this dissertation is a product of research work undertaken by myself. It has neither been in part or being presented elsewhere for another degree.

SIGNED.....

DATE.....

PEARL AMA ADOMAH ESSEL

(STUDENT)

SIGNED.....

DATE.....

REX GYEABOUR ABREFAH (PhD)

(SUPERVISOR)

SIGNED.....

DATE.....

HENRY CECIL ODOI (PhD)

(CO-SUPERVISOR)



ABSTRACT

Ghana is in the process of converting its fuel from Highly Enriched Uranium (HEU) to Lowly Enriched Uranium (LEU) even though the HEU fuel is not fully spent, thus the handling of the irradiated fuel is in the offing. Irradiated fuel consists of radioactive fission and activation products generated in the nuclear fuel which are hazardous to personnel, environment and the public. As a result, the knowledge of the dose rate will aid in safe guarding the process of core conversion. Two computer codes used to carry out this research work were ORIGEN-S; for computing changes in the isotopic concentrations during neutron irradiation and radioactive decay as well as to determine the source term and MCNP6; which used the source term estimated by the ORIGEN-S code to calculate the dose rate in mrem using point detectors and also to determine the criticality of the core at different heights above the bottom of the core in order to mimic the process of unloading the core. Most of the radionuclides present after the core depletion contributed to the source term of 1.767×10^{13} photons/sec which was observed after thirty days of the cooling period. The dose rates ranged between 3.51×10^{-25} mGy/hr and 4.27×10^4 mGy/hr with the detectors placed at positions above the reactor core, the control room (wall, door and window) and the rabbit room. The criticality (k_{eff}) also decreased from 0.99442 to 0.01238 which indicates that the nuclear fuel will remain sub critical. The results proved that the core unloading will be done safely.

DEDICATION

This is dedicated to my God and family for their support throughout my study. Also, to everyone who helped me in diverse ways during my research work, you are special.



ACKNOWLEDGEMENTS

I am grateful to the Jehovah God for His guidance, grace and protection throughout this course.

With sincere gratitude, I say Jehovah bless all my lecturers for their input, relentless effort and support through my research work. A special one to my supervisors Dr. Rex Gyeabour Abrefah and Dr. Henry Cecil Odoi not forgetting Prof. J.J Fletcher for their expert guidance, advice and encouragement.

I am also grateful to the staff of the Argonne National Laboratory, Argonne, U.S.A, for their support in running my codes.

Last but not the least I am indebted to my family, colleagues, friends and my course mates whose support cannot go unnoticed.

I am forever grateful. God bless you all

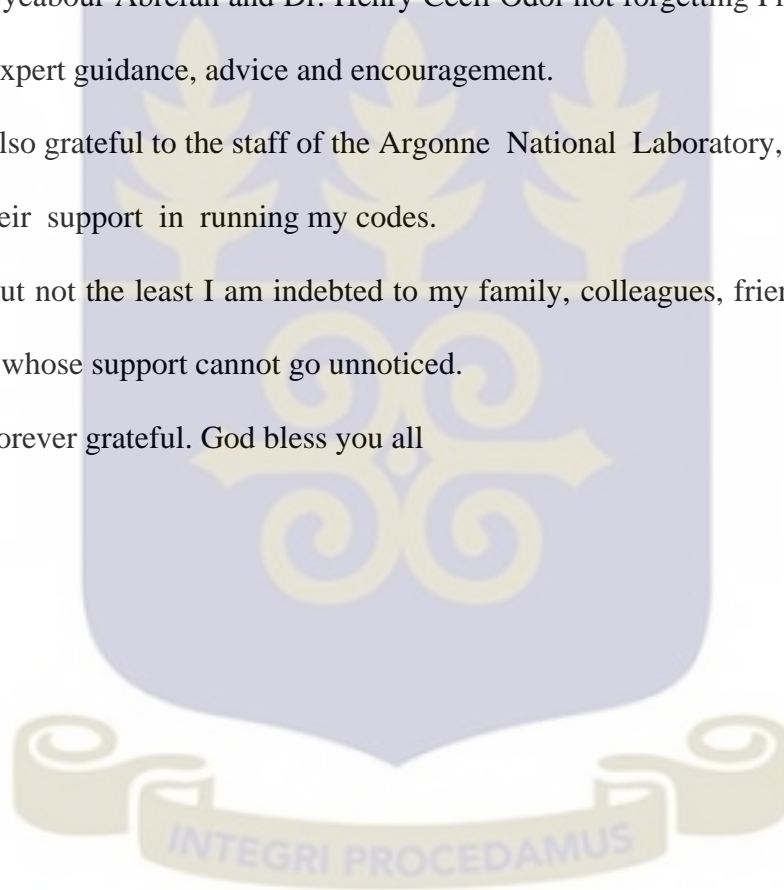


TABLE OF CONTENTS

DECLARATION	i
ABSTRACT.....	iii
DEDICATION.....	iv
ACKNOWLEDGEMENTS.....	v
TABLE OF CONTENTS.....	vi
LIST OF TABLES.....	x
LIST OF SYMBOLS	xii
LIST OF FIGURES	xiii
LIST OF ABBREVIATIONS.....	xv
CHAPTER ONE.....	1
1 INTRODUCTION.....	1
1.0 BACKGROUND	3
1.1 PROBLEM STATEMENT	7
1.2 OBJECTIVES.....	7
1.3 JUSTIFICATION.....	8
1.4 SCOPE OF WORK	8
1.5 STRUCTURE OF WORK.....	9

CHAPTER TWO	11
2 LITERATURE REVIEW.....	11
2.0 National Nuclear Security Administration (NNSA).....	11
2.1.0 The Portuguese Research Reactor (RPI).....	13
2.1.1 Jamaican SLOWPOKE core conversion.....	14
2.1.2 Budapest Research Reactor (Hungary)	18
2.1.3 China to convert micro-reactor	21
2.2 CODES EMPLOYED BY OTHER RESEARCHER	22
2.2.0 Dose Analysis for Spent fuel transport using UNF-ST&DARDS.....	23
2.2.1 Photon dose rate from SNF of Material Testing Reactor (MTR)	23
2.2.2 Mass Inventory of Spent Fuel of Research Reactors	24
2.3 Ghana Research Reactor-1 (GHARR-1)	28
CHAPTER THREE	33
3 THEORY.....	33
3.0 ORIGEN-S.....	33
3.0.1 SOLUTION WITH THE MATRIX EXPONENTIAL METHOD	36
3.0.2 SOLUTION TO THE NUCLIDE CHAIN EQUATIONS.....	41
3.0.3 PHOTON SOURCES AND SPECTRA	44
3.0.4 TIME DEPENDENCE OF THE NEUTRON FLUX	46
3.1 MCNP6.....	48

3.1.0	PARTICLE TRACKS	50
3.1.2	CRITICALITY CALCULATIONS	52
CHAPTER FOUR.....		54
4	METHODOLOGY.....	54
4.0	ORIGEN-S.....	54
4.0.1	Determination of source term and isotopic inventory.....	55
4.1	MCNP.....	57
4.1.0	GHARR-1 MCNP model	58
4.1.1	Analysis of GHARR-1 MCNP simulated results.....	58
4.1.2	Dose estimation using MCNP6.....	59
CHAPTER FIVE		67
5	RESULTS AND DISCUSSION	67
5.0	CORE INVENTORY OF NUCLEAR FUEL OF GHARR-1.....	67
5.0.1	Source term estimation.....	72
5.1	RADIATION DOSE RATE AND CRITICALITY FROM MCNP.....	73
5.1.0	Results from MCNP6 dose rate estimation.....	74
5.1.1	Criticality (k_{eff}) calculations.....	81
CHAPTER SIX.....		83
6	CONCLUSION AND RECOMMENDATION.....	83
6.0	CONCLUSION	83

6.1 RECOMMENDATION.....	85
REFERENCES	87
APPENDIX.....	93
Appendix A.1 Gamma Source intensity during the decay period	93
Appendix A.2 39 SOSNY Specified Gamma Energy Groups (MeV)	97



LIST OF TABLES

Table 2.1: Comparison of Key Parameters for GHARR-1 HEU and LEU Cores	27
Table 5.1: Inventory of some important radionuclides in the Actinide group	68
Table 5.2: Inventory of some important radionuclides in the Light Element group	69
Table 5.3: Inventory of some important radionuclides in the Fission Products group ...	70
Table 5.4: Gamma source intensity during the cooling cycle after shut down	72
Table 5.5: Dose rate at various heights above the bottom of core with detector above the reactor floor.....	75
Table 5.6: Dose rate at various heights above the bottom of core with detector towards the control room.....	75
Table 5.7: Dose rate at various heights above the bottom of core with detector away from the control room.....	76
Table 5.8: Dose rate at various heights above the bottom of core with detector towards the door	76
Table 5.9: Dose rate at various heights above the bottom of core with detector at the door	77
Table 5.10: Dose rate at various heights above the bottom of core with detector at the Control room window	77
Table 5.11: Dose rate at various heights above the bottom of core with detector at the Rabbit room window.....	78
Table 5.12: Dose rate at various heights above the bottom of core with detector at the Far side of room	78

Table 5.13: Dose rate at 595cm above the bottom of core with detector placed at different positions 79

Table 5.14: Criticality values as the cage is being lifted to the top of the vessel..... 82



LIST OF SYMBOLS

N_i = atom density of nuclide i,	34
λ_i = radioactive disintegration constant of nuclide i,.....	34
σ_i = spectrum-averaged neutron absorption cross section of nuclide i,.....	35
Φ = space- and energy-averaged neutron flux,	35
l_{ij} = branching fractions of radioactive disintegrations from other nuclides j,	35
f_{ik} = branching fractions for neutron absorption by other nuclides k that lead to the formation of species i.....	35
E_a = actual photon energy (MeV),	45
E_g = mean energy of the group (MeV),	45
I_g = group photon intensity (photons per disintegration).....	45
$Q(\mathbf{r}', \nu)$ = source term	49
$C(\nu' \rightarrow \nu, \mathbf{r}') =$ collision kernel, change velocity at fixed position \mathbf{r}'	49
$C(\mathbf{r}' \rightarrow \mathbf{r}, \nu) =$ transport kernel, change in position \mathbf{r} at a fixed velocity ν	50
Angular Flux = $\Psi(\mathbf{r}, \nu) = \frac{\Psi(\mathbf{r}, \nu)}{\Sigma(\mathbf{r}, \nu)}$	50
Scalar Flux = $\phi(\mathbf{r}, \nu) = \int_{\Omega} \frac{\Psi(\mathbf{r}, \nu)}{\Sigma(\mathbf{r}, \nu)} d\vec{\Omega}$, where, $\nu = \nu \vec{\Omega}$	50
Solid Angle = $\overline{d\Omega}$	50
$S(\mathbf{r}, \nu) =$ Fixed source term	50
$F(\nu' \rightarrow \nu, \mathbf{r}) =$ creation operator (due to fission), particles at (\mathbf{r}, ν') creates particles at (\mathbf{r}, ν)	50
$K =$ eigenvalues	50

LIST OF FIGURES

Fig. 1: A once through (or open) fuel cycle.....	6
Fig 2.1: Cross- sectional view of the JM-1 core	15
Fig 2.2: Top view of the Reactor core	15
Fig 2.3: Reactor cage of JM-1 being lifted	16
Fig 2.4: JM-1 LEU core cross section with power distribution and coolant channels segmentation	16
Fig 2.5: A vertical cross section of JM-1 as modeled with MCNP5	17
Fig 2.6: A horizontal cross section of the JM-1 MCNP5 model	17
Fig 2.7: A view of the reactor hall	19
Fig 2.8: Scientist on top of the reactor.....	19
Fig 2.9: Budapest Research Reactor	20
Fig 2.10: The process of core removal.....	20
Fig 2.11: Hungary completes core conversion and core safely stored in a cask ready for transportation	21
Fig 2.12: Core of the China Research Reactor	22
Fig. 2.13: The MNSR Research Reactor	28
Fig 2.14: MCNP plot of the core configuration and associated experimental channels..	31
Fig 2.15: MCNP plot of vertical cross-section of GHARR-1 reactor (in full power mode)	31
Fig 4.1: Flow chart illustrating methodology	62
Fig.4.2: Fuel Cage Center at the bottom of core 0.0 cm.....	63
Fig. 4.3: Fuel Cage Center at 24.6 cm above bottom	63

Fig.4.4: Fuel Cage Center at 240 cm above bottom 64

Fig.4.5: Fuel Cage Center at 480 cm above bottom 64

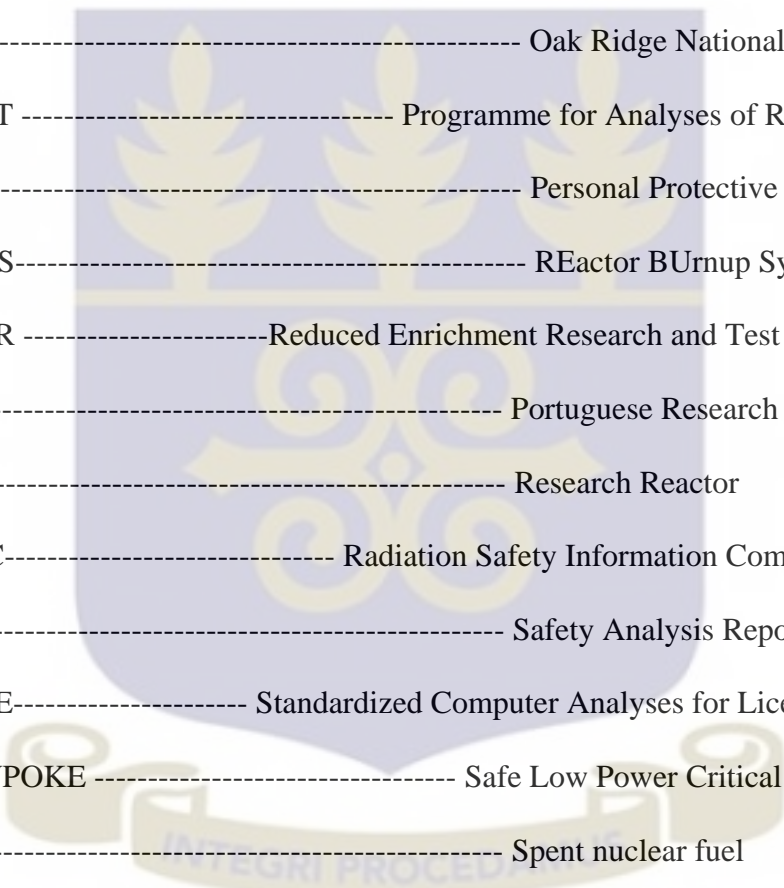
Fig.4.6: Fuel Cage Center at 495 cm above bottom 65

Fig. 4.7: Fuel Cage Center at 595 cm above bottom 65



LIST OF ABBREVIATIONS

ALARA	As Low As Reasonably Achievable
ANL	Argonne National Laboratory
BRR	Budapest Research Reactor
CRP	Coordinated Research Project
DoE	Department of Energy
ENDF	Evaluated Nuclear Data File
FP	Fission Products
GAEC	Ghana Atomic Energy Commission
GHARR-1	Ghana Research Reactor -1
GTRI	Global Threat Reduction Initiative
HEU	Highly Enriched Uranium
HLW	High Level Waste
IAEA	International Atomic Energy Agency
ILW	Intermediate Level Waste
JM- 1	Jamaican SLOWPOKE reactor
LE	Light Elements
LEU	Low Enriched Uranium
LLW	Low Level Waste
M ³	Materials Management and Minimization
MCNP	Monte Carlo N- Particle
MNSR	Miniature Neutron Source Reactors
MTR	Material Test Reactor



MTU	Metric tons of Uranium
MW	Mega Watts
NF	Nuclear Fuel
NNSA	National Nuclear Security Administration
NRA	Nuclear Regulatory Authority
ORIGEN	Oak Ridge Isotope GENERation
ORNL	Oak Ridge National Laboratory
PARET	Programme for Analyses of Reactor Transients
PPA	Personal Protective Apparel
REBUS	REactor BUrnup System
RERTR	Reduced Enrichment Research and Test Reactor Program
RPI	Portuguese Research Reactor
RR	Research Reactor
RSICC	Radiation Safety Information Computational Center
SAR	Safety Analysis Report
SCALE	Standardized Computer Analyses for Licensing Evaluation
SLOWPOKE	Safe Low Power Critical (K) Experiments
SNF	Spent nuclear fuel
TLD	Thermo Luminescent Dosimeter
UF	Uranium hexafluoride
UNF-ST&DARDS	Used Nuclear Fuel Storage, Transportation & Disposal Analysis Resource and Data System
US	United States

U-Al₄ ----- Uranium-Aluminium

UO₂ ----- Uranium Oxide

Zirc-4 ----- Zircaloy-4



CHAPTER ONE

1 INTRODUCTION

As of June 2015, the International Atomic Energy Agency's (IAEA) Research Reactors (RRs) database had 672 RRs of which 274 are operational in 56 countries. Out of this, 89 of them are in 39 developing countries. 214 have been shutdown and 168 have been decommissioned with 16 under construction or are planned for the future. [1]

Although many of the RR have been shutdown and there is also a fall in the number of new RRs being brought into operation, it does not make RRs unnecessary as the new one are innovative, multipurpose reactors designed to produce high neutron fluxes that will meet the nuclear research and development needs of the countries in which they are being built. [1]

While a few old reactors give reasons for safety concerns, majority have been renovated at least once so that their key components meet modern safety and technological standards. The thermal power distribution of operating RRs indicates that large fractions are less than 5MW (that is about 77%). Research Reactors of less than 100kW operates with a lifetime core and as such no spent fuel arises until they are permanently shut down. The current core of Ghana Research Reactor -1 (GHARR-1) reactor which is less than 100kW is near the process of being converted from Highly Enriched Uranium to Low Enriched Uranium [1].

Research reactors possess unique challenges in the back end of the fuel cycle because many different designs using a large variety of fuel types have been built, often for special purposes. These include the management of experimental and exotic fuels with no plan of reprocessing, and significant numbers of fuel assemblies that failed in

their reactors or were subsequently corroded in wet storage. Similarly the variety of designs poses special challenges for decommissioning.

Several numerical and computational methods or approaches based on nuclear reactor physics, nuclear engineering, depletion codes and mathematical theories exist for performing core depletion analysis and particle transport analysis [2].

Over the years, both deterministic and stochastic methods have been employed in the performance of analysis of particle transport. With the advent of advanced, powerful and sophisticated computers, innovative methods involving the extensive use of Monte Carlo-based computational codes or tools and large scale computing facilities have now been adopted in analyzing complex nuclear and radiation transport processes. In particular, previous models and codes which were hitherto limited to running on low-speed computers, have also been improved and can now be adapted to performing equally time-demanding simulations and calculations [3] [4]. With improved mathematical and numerical computational methods, analyses of particle transport have even become more involving howbeit challenging in time, space and energy.

On the other hand, the use of depletion codes is very important in the calculation of dose rate in various systems. Several depletion codes exist that can be used to deplete reactor core in order to achieve radionuclides inventory and source term. ORIGEN-S is a readily available tool which uses matrix exponential methods to solve a large system of differential equations.

During a nuclear reaction in a reactor, new radionuclides fragments are formed together with neutron and the release of heat energy. The fission products undergo beta decay and forms daughter radionuclides. These radionuclides have the ability to absorb neutrons and

are referred to as poisons. The continuous absorption of these neutrons leads to a reduction of the reactivity (used to describe the deviation of a reactor's criticality from unity with time). This eventually leads to the inability of the fuel to sustain a nuclear chain reaction. The nuclear fuel (NF) is therefore termed Spent Nuclear Fuel (SNF).

The neutrons may be absorbed by the fuel materials to continue the fission process with the production of two or more neutrons or by the radionuclides thereby reducing the population of neutrons.

Nuclear power is becoming an ever more significant part of the energy programmes of many countries. At the back end of the fuel cycle, the spent nuclear fuel is a huge challenge reactor operator's encounter. This must be safely removed, transported, stored and managed well pending its reprocessing or disposal. Spent fuel management is one of the most vital and common problems for countries with reactors. It also invokes the concern of the public at large [5].

Ghana has no plans or facilities for permanent storage yet. The option that is available to Ghana now which is the open nuclear fuel cycle scenario where the manufacturers of the core would take back the spent nuclear fuel for its management. In the closed nuclear fuel cycle, further fuel storage capacity may be required to match the increasing spent fuel with the available capacity of reprocessing plants.

1.0 BACKGROUND

The program to convert research reactors from the use of highly enriched uranium (HEU) to low enriched uranium (LEU) started under the U.S. Department of Energy (DOE) with the RERTR (Reduced Enrichment for Research and Test Reactors) in 1978

In 2004 the DOE's National Nuclear Security Administration (NNSA) established the Global Threat Reduction Initiative (GTRI) that incorporated the reactor conversion program as one of the main pillars for HEU minimization. GTRI was recently restructured to be part of a new office known as Material Management and Minimization (M³) in January 2015 with the mandate to address the persistent threat posed by nuclear materials through a full cycle of materials management and minimization efforts. The primary objective of M³ is to achieve permanent threat reduction by minimizing and, when possible, eliminating weapons-usable nuclear material around the world [6]

In all, thirty-nine (39) Research reactors had converted to LEU by 2004 with eleven (11) of these reactors in the U.S. and the remaining twenty-eight (28) in foreign countries. GTRI has accelerated the program to minimize HEU utilization in civil applications. Seventy-six (76) research reactors have converted to date or have shutdown before conversion, twenty (20) of these reactors are in the U.S. and the remaining fifty-six (56) are in foreign countries.

The estimated reactor parameters exhibited very good agreement with experimental data and the results was in better agreement than all previously reported estimates for both the HEU and LEU cores after the neutronic analysis were done. [2][7]

Ghana's Nuclear Fuel is in poll position to be converted from Highly Enriched Uranium (HEU) to Lowly Enriched Uranium (LEU) even though our fuel is not fully spent.

The call by the international community to convert nuclear fuel from HEU to LEU due to nuclear weapon proliferation has been welcomed by Ghana and thus the need to convert the nuclear fuel although it is not completely spent. The process of converting NF will thereby make handling of the irradiated fuel imminent.

Spent fuel and other high-level radioactive waste are extremely hazardous, although nuclear research reactors produce relatively small volumes of waste compared to other power plants because of the high energy density of nuclear fuel.

The radioactive constituent of SNF waste is a factor that determines the classification of the waste. There are six classes used as the basis for the classification of radioactive waste according to IAEA. These six classes are the Exempt waste, Very short lived waste, Very Low level waste, Low Level waste, Intermediate Level waste and the High level waste.

All these classes of nuclear wastes have their own separate radiation levels which also determine the extent of harm that can occur when one gets in contact with it.

Nuclear Fuel (NF) from Ghana Research Reactor-1 (GHARR-1) falls under the Intermediate-level waste (ILW) because of its content particularly of long lived radionuclides which requires a greater degree of shielding than that provided by near surface disposal and needs no provision, or only limited provision, for heat dissipation during its handling, transportation and interim storage. ILW may contain long lived radionuclides, in particular, alpha emitting radionuclides that will not decay to a level of activity concentration acceptable for near surface disposal during the time for which institutional controls can be relied upon. Therefore, waste in this class requires disposal at greater depths, of the order of tens of meters to a few hundred meters. [8]

Currently there are three basic fuel management methods. The wait and see method where countries continue to evaluate their back end strategy while in the meantime taking intermediate step (this is the most common approach used). The closed cycle is the

second method, where there is reprocessing of the spent fuel and recycling of plutonium and uranium in the form of mixed oxide. The open (once-through also known as the throw away) cycle is the last but not the least, in this cycle, the nuclear material (fuel) passes through the reactor just once. After irradiation, the fuel is kept at the reactor site in a transfer cask until it is sent away from the reactor site for disposal. (GHARR-1 spent fuel falls under this category) [9] [10]. Figure 1 shows a diagram of the open type of fuel management.

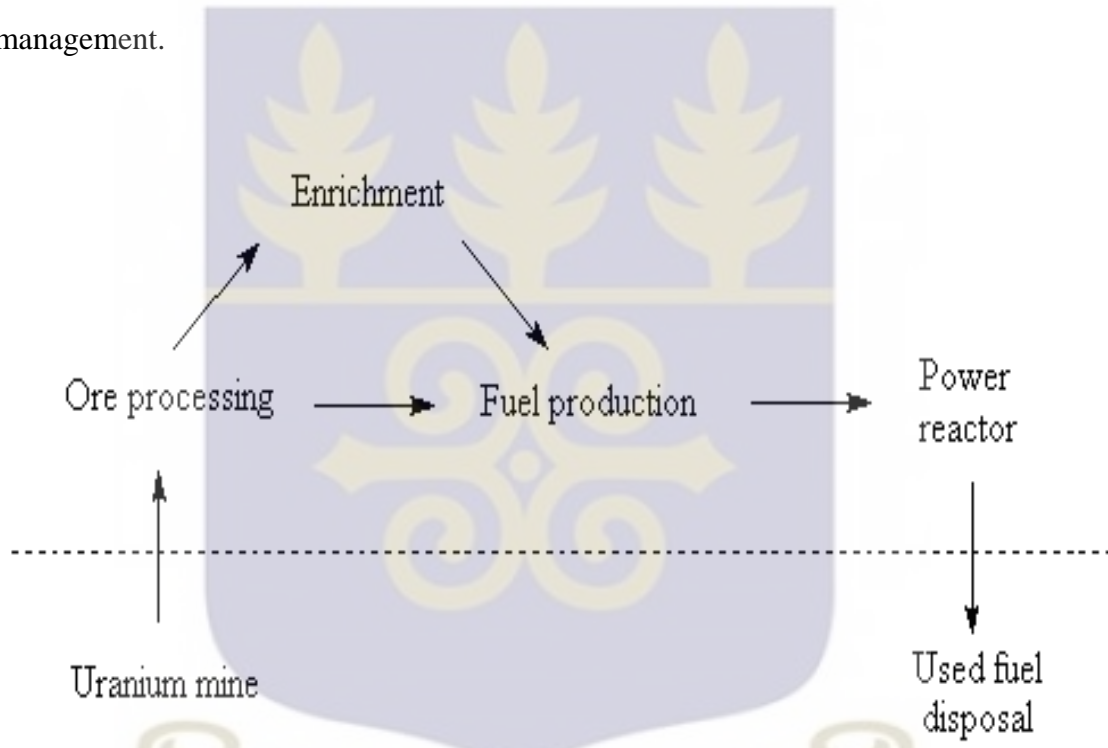


Fig. 1: A once through (or open) fuel cycle

[10]

It is against this background that this study seeks to determine the radiation exposure to personnel involved in the core conversion, the general public and the environment. The dose rate will be estimated to help manage doses to personnel, the general public and the environs during and after the Core Conversion in that the conversion will pose no threat to lives.

1.1 PROBLEM STATEMENT

The composition of nuclear fuel is fission products, actinides and activation elements. The components transmute by beta and gamma decay into other daughter radionuclides which could be very harmful to the body. The transmutation also results in the release of neutrons and photons. These particles can be harmful when certain limits are exceeded. It is imperative to protect the personnel, public and environment from their effect.

Furthermore the requirement for procuring a license from the Nuclear Regulatory Authority is to prove that the process of core conversion will be safe. The dose rate calculations and radionuclide inventory obtained as a result of this work will help the Ghana Nuclear Regulatory Authority (NRA) to issue a license for the core conversion in the calculations of the cask needed to house the used Nuclear Fuel for its transportation.

1.2 OBJECTIVES

This study is a vital one to the safety assessment of the reactor. The aims of the study are as follows

1. To determine core inventory of the spent nuclear fuel
2. To evaluate the Source Term
3. To determine the dose rate at specific points along the length of the reactor vessel during the core removal
4. To determine the k_{eff} (to know criticality) at various levels so as to maintain the SNF at a sub critical level

1.3 JUSTIFICATION

The core conversion has reached its implementation stage. This stage includes the unloading of HEU core from the reactor vessel. In bringing out the cage from the vessel, the determination of the dose rate emanating from the fuel as well as the amount of neutrons present is key to this core conversion activity. As the core is moved out of the reactor vessel, the photons and actinides as well as the other fission product that are released should be As Low As Reasonable As Achievable (ALARA).

This work seeks to determine the dose rate so as to help in putting in place the proper measures during unloading of the core. The type of shielding to be adopted as well as the correct Personal Protective Apparels (PPAs) to be used will be obtained.

The results from this work will be used in documentation for good records keeping. It will also serve as a starting point for future research works.

This research work is a very important one as the operators of the reactor seek approval from the Nuclear Regulatory Authority (NRA).

1.4 SCOPE OF WORK

It is well-known that radioactive fission and activation products generated in nuclear fuel constitute the principal source of hazard to personnel, environment and public. As a consequence, determining the dose rate will be done to evaluate fission product released from GHARR-1. A mechanistic approach to evaluating releases with sufficient accuracy is a complex and nerve-racking task. Fortunately, for most applications of practical interest, non-mechanistic, empirically based approaches (correlations) are adequate. Such approaches may be employed directly through manual calculations or implemented in system codes for evaluation of the source term and releases to the environment [2].

Two computer codes, ORIGEN-S and MCNP6 were used. ORIGEN-S is used for computing changes in isotopic concentrations during neutron irradiation and radioactive decay as well as the source term calculation.

MCNP6 uses the source term estimated by the ORIGEN-S code to calculate the dose rate in mrem using point detectors.

The criticality of the cage as well as the dose rate with respect to the cage was taken at different distances (that is 0, 24.6, 240, 480, 495 and 595 all in cm) from the bottom of the core in order to mimic the process of unloading the core. The effect of the photons and neutrons emanating from the core at different distances from the bottom of the core is analysed. The dose rates at various points in the reactor hall and reactor building when the core is out of the reactor vessel and hanging in air will be obtained and analysed.

1.5 STRUCTURE OF WORK

Chapter one will focus on the Introduction to the work. It also looks at the problem that this work is trying to solve, the objectives and the justification for this work.

Chapter two contains the literature review which generally looks at what research work has already been done in the field of dose rate calculation during core conversion. The advantages of my work and other works will be analysed.

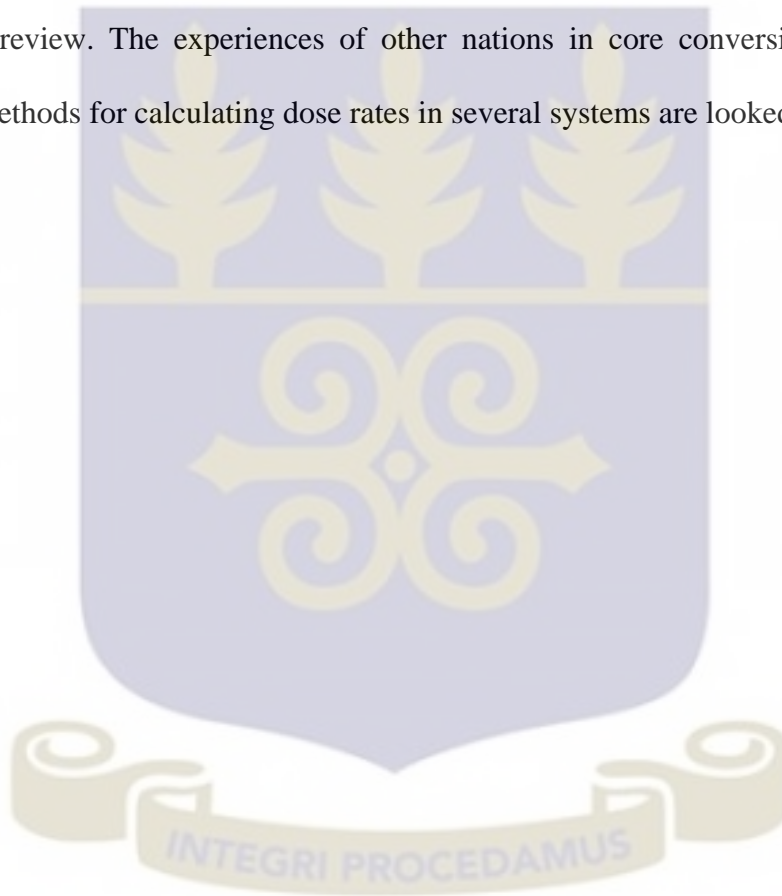
Chapter three will focus on the fundamental theory used in developing the codes.

Chapter four outlines the methodology in solving the problem. It shows clearly what processes and procedures were used to attain the results.

The results obtained in the previous chapter will be discussed in chapter Five.

Conclusions and recommendations based on the results obtained and discussed in chapter five will be made in chapter Six.

Chapter One gave a general overview Research Reactors, the type of waste and the management of GHARR-1's Nuclear Fuel, the purpose of this work and a general overview of the codes employed in this research. The next chapter focuses on the literature review. The experiences of other nations in core conversion are examined. Several methods for calculating dose rates in several systems are looked at.



CHAPTER TWO

2 LITERATURE REVIEW

The general description of the GHARR-1 reactor is outlined in this chapter. The efforts made by the National Nuclear Security Administration (NNSA) at formulating programs to facilitate the core conversion project are also looked discussed in this chapter. The various core conversion programs by the NNSA and a few countries that have successfully converted their reactors core will be discussed. Radiation dose calculation as well as inventory of Spent Nuclear Fuel performed by other researchers will also be discussed.

2.0 National Nuclear Security Administration (NNSA)

The program to convert RRs from the use of highly enriched uranium (HEU) to low enriched uranium (LEU) started under the U.S. Department of Energy (DOE) with the RERTR (Reduced Enrichment for Research and Test Reactors) in 1978. In 2004, the Global Threat Reduction Initiative (GTRI) program was established to replace the RERTR to implement the US policy of minimizing and eliminating the use of highly enriched uranium (HEU) in civilian applications by working to convert research and test reactors to the use of low enriched uranium (LEU). Finally GTRI become part of the Office of Materials Management and Minimization (M³ office) which was established in 2015. M³'s focus is to convert-remove-dispose which is different from GTRI's mandate of convert-remove-secure.

The core conversion program requires that the reactor's safety, performance and operations should not be significantly affected after the conversion. Due to these constraints of maintaining the reactors operational characteristics, safety and performance, the expected timeline for completion in 2018 has been projected to 2035 to give way for further preliminary feasibility studies to be done.

GTRI Conversion program focused on both US research reactors and foreign reactors. In the U.S., all reactors that could convert with existing fuel have been converted. Foreign reactor conversion program under GTRI has made very significant progress in the conversion of Russian supplied reactors.

Current core conversion efforts continue with other US supplied foreign reactors and the remaining Russian supplied reactors as well as LEU fuel qualification and conversion of high flux reactors in Europe. Chinese supplied reactors (MNSRs) and the initiation of feasibility studies for the conversion of specific Russian domestic reactors.

The core conversion is aimed at developing or identifying an alternative LEU fuel assembly with a service lifetime at least similar to that of the HEU fuel assembly to ensure that safety criteria are satisfied. GTRI ensures that the core conversion can be achieved without requiring major changes in reactor structures or equipment. It also determines, as possible, that the overall costs associated with the conversion do not increase significantly the annual operating costs [7] [11].

In 2006, the IAEA put together all the MNSR Operating Countries to undertake a Coordinated Research Project (CRP) that will ascertain the feasibility of replacing the High Enriched Uranium (HEU) fuel of the Reactor with Low Enriched Uranium (LEU). This CRP was successfully completed in March 2012 after various meetings were held to

discuss results and prepare the way forward. Subsequently, a Working Group was formed to monitor the progress of the various MNSRs Conversion Activities and to share lessons learnt with each other. Current effort is toward conversion of Chinese-supplied MNSR reactor to countries such as Nigeria, Ghana, Pakistan, Iran, and Syria through the IAEA Coordinated Research Project (CRP).

2.1.0 The Portuguese Research Reactor (RPI)

Core conversion of the Portuguese Research Reactor (RPI) to LEU fuel is being performed within the IAEA Technical Cooperation project POR/4/016, with financial support from the U.S. and Portugal. The RPI is a 1 MW pool-type reactor commissioned in 1961. It is owned and operated by “Instituto Tecnológico e Nuclear”, which is the third generation of the main national organisation for nuclear activities in Portugal. It was built by AMF Atomics during the period of 1959-61 in the then “Laboratory for Nuclear Physics and Engineering” (LFEN in Portuguese). Its design follows closely the one of the Battelle Research Reactor. It started up using LEU fuel but a decision to convert it to HEU fuel was taken in the early seventies for economic reasons. Its fuel was converted to HEU in 1990 after a refurbishment of the reactor at a time when the conversion to LEU fuel was already being addressed in many research reactors. The declaration at the end of 2004 of the 10 year extension on the U.S. foreign research reactor spent fuel acceptance policy opened a new window of opportunity for the operation of the RPI with LEU fuel again. The safety analyses for the core conversion were made with the assistance of the GTRI Conversion program and were submitted for regulatory approval in January 2007.

The results of neutronic studies, steady-state thermal-hydraulic analyses, accident analyses, and revisions to the Operating Limits and Conditions demonstrate that the RPI

can be operated safely with the new LEU fuel assemblies. The main results were presented in the RERTR conference in 2006. The detailed safety studies took longer than originally foreseen. While for the neutronic studies all information was readily available and a very basic MCNP model existed, additional information was needed on the reactor thermal-hydraulics parameters, taking into account the somewhat limited studies performed earlier for the conversion to HEU. The core was finally converted and the spent fuel shipped in 2008 [12]

2.1.1 Jamaican SLOWPOKE core conversion

Jamaican finally completed the conversion of the core of its reactor in September 2015. The reactor is a SLOWPOKE research reactor with rated power of 20 kW supplied by the Atomic Energy of Canada Limited (AECL). Its fuel which is approximately 1kg was made of 93% U235 enrichment of HEU supplied by the U.S through a Project and Supply Agreement with the IAEA. The reactor achieved its first criticality in March 1984 and normally operated at an average power of 10 kW for approximately 1300 hours per year. With the call by the international bodies, a request was made in 2009 through the IAEA to the GTRI and the Reduced Enrichment for Research and Test Reactors (RERTR) program to convert the reactor in Jamaica to LEU fuel in order to achieve the global threat reduction initiative and the growing international consensus to eliminate civil uses of HEU. The AECL under the GTRI have developed LEU fuel fabricated from zircaloy-4 clad uranium oxide pellets and contained 1100g of 19.9% U235 (total mass of U ~5600g) enrichment of LEU fuel. The estimated reactor neutronic and thermal hydraulic parameters were performed using MNCP5 computational model. Results were in good agreement for both the HEU and LEU cores [13] [14].

Some images of the Jamaican HEU fuel reactor and the process of core conversion are shown in fig 2.1 to 2.6:



Fig 2.1: Cross- sectional view of the JM-1 core

[15]

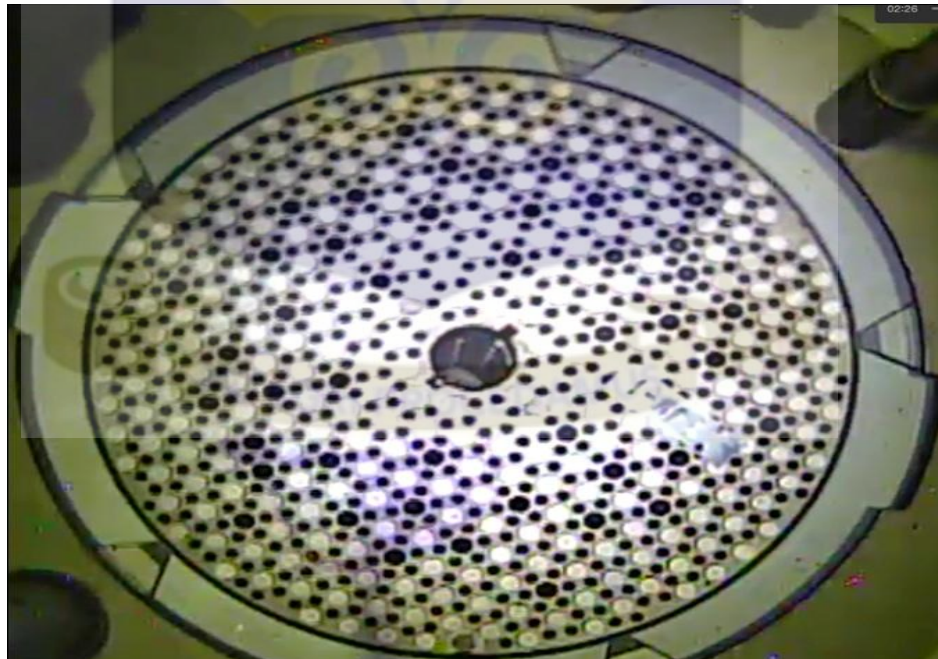


Fig 2.2: Top view of the Reactor core

[15]



Fig 2.3: Reactor cage of JM-1 being lifted

[15]

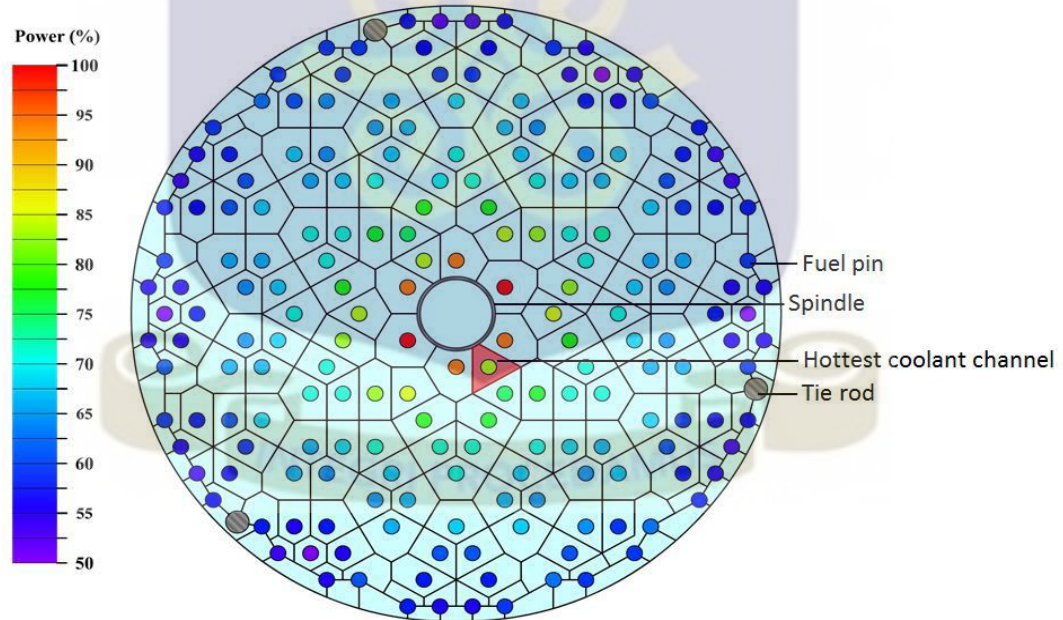


Fig 2.4: JM-1 LEU core cross section with power distribution and coolant channels segmentation

[16]

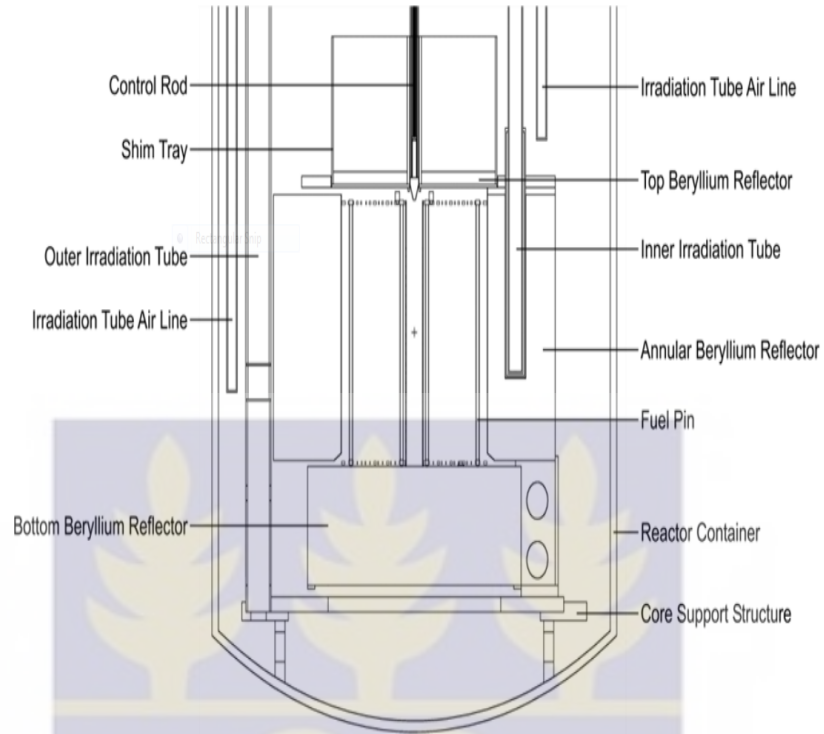


Fig 2.5: A vertical cross section of JM-1 as modeled with MCNP5

[16]

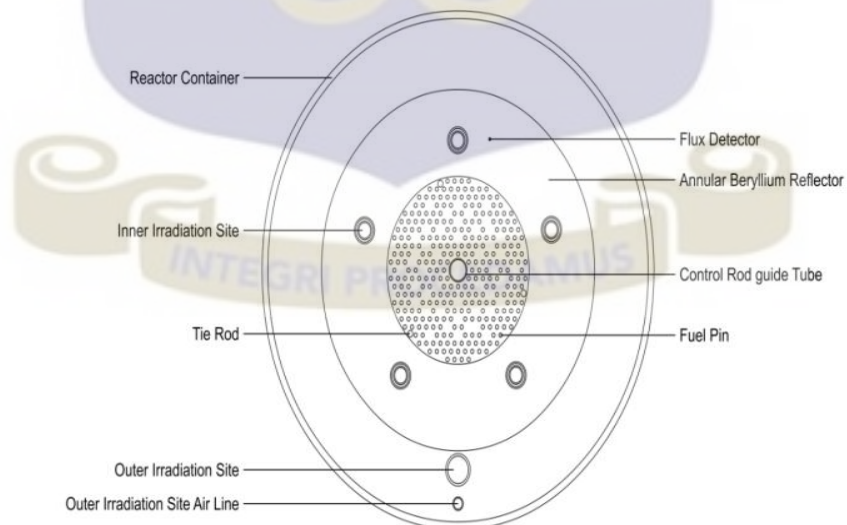


Fig 2.6: A horizontal cross section of the JM-1 MCNP5 model

[16]

2.1.2 Budapest Research Reactor (Hungary)

The Budapest Research Reactor (BRR) is a WWRS-M10 Soviet designed tank type, water cooled and water moderated thermal neutron reactor. It had an initial power of 2MWth and attained its first criticality in 1959.

It was first modified to increase the power to 5MWth with a change of fuel to 36% enriched fuel. Later the power was increased to 10MWth with its System, Subsystem and Components (SSCs) replaced. The 10MWth received its license in 1993. Since its restart, the reactor has performed 64,000 hrs with 26GW days.

The reactor physical calculations were made with the KIKO3D program and were validated by ANL DIF3D program. The KIKO3D reactor dynamic program was used for the safety analyses of reactivity transients. Applying this program was acceptable for the type of reactivity incident/anomaly when the power distribution change on both radial and axial directions. During the calculation the time dependent diffusion equation was solved by nodal method in 3D

In parallel with the KIKO3D, the ATHLET thermo hydraulic program was run which determined the coolant agent density and temperatures. The MULTICELL program gave the nuclear particle's parameters (nuclear group factors) for the KIKO3D. The WIMS software was used for the DIF3D program. The changing and the supplementation of the fuel handling procedures were also performed.

The final results of the calculations and the iterations performed satisfied the requirements. The length of cycles and the reactor time table was the same as it was earlier.

The core conversion was completed successfully and all planned tasks were performed. There was no significant deviation in neutron flux distribution; the control rod reactivity worth remained the same. [17] [18]



Panorama view of the Reactor Hall

Fig 2.7: A view of the reactor hall

[19]



Fig 2.8: Scientist on top of the reactor

[19]



Fig 2.9: Budapest Research Reactor

[19]



Fig 2.10: The process of core removal

[19]



Fig 2.11: Hungary completes core conversion and core safely stored in a cask ready for transportation

[19]

[20] [21]

2.1.3 China to convert micro-reactor

The Miniature Neutron Source Reactor (MNSR) Prototype is the first Chinese reactor to be converted to LEU through international collaboration. The conversion program reduces the proliferation concern of reactors fueled with high enriched uranium (HEU). The MNSR Prototype conversion was accomplished with U.S. technical assistance under the auspices of NNSA's Office of M³ reactor conversion program, which has converted or verified shutdown of more than 90 HEU-fueled research and test reactors worldwide over the past 30 years.

Argonne's team of experts in neutronics, thermal-hydraulics and materials worked with their Chinese counterparts to redesign the reactor core to contain a more dense fuel paired

with structural materials that absorb fewer neutrons, thereby allowing the reactor to operate in the same parameters with the LEU fuel. [7]



Fig 2.12: Core of the China Research Reactor

[7]

2.2 CODES EMPLOYED BY OTHER RESEARCHER

There are several methods of assessing the radiation dose received by the public and workers. Some of the methods are based on computer codes, estimates using assumed scenarios, calculation of dose rates from the spent fuel properties and also data from direct measurements. Some of the computer codes and the cases in which they were used are elaborated below.

2.2.0 Dose Analysis for Spent fuel transport using UNF-ST&DARDS

Used Nuclear Fuel Storage, Transportation & Disposal Analysis Resource and Data System (UNF-ST&DARDS) was employed by Georgeta Raulescu et al to compute dose analysis for Spent Fuel. It's an integrated data and analysis system that facilitates automated casks specific analyses based on actual characteristics of the as-loaded SNF. The codes used were the ORIGAMI (ORIGen AsseMbly Isotopics) and MAVRIC (which is a Scale shielding calculation sequence) which are part of Scale 6.2. The ORIGAMI was used in the radiation source term estimation and the MAVRIC for the dose calculation. The dose rates at locations of interest will be significantly lower than the dose rate limits in 2025 and beyond as stated in the NRC's Packaging and Transportation of Radioactive Materials (10 CFR 71) regulatory dose rate limits. The dose rate values corresponding to year 2025 as projected were between 4 and 12 times lower than the regulatory dose rate limit of 10mrem/h. [22]

2.2.1 Photon dose rate from SNF of Material Testing Reactor (MTR)

The photon dose rate from spent fuel assemblies of a typical MTR was calculated for the purpose of estimating the radiation level. The dose rate data are evaluated as functions of specific power density and burnup in the fuel assembly and as a function of fission product decay time in the spent fuel. The fuel assembly had Aluminum-clad fuel plates with aluminum side plates

The fission product photon source was calculated using the isotope generation and depletion code, ORIGEN. The source was calculated for a ^{235}U mass with up to 80% burnup and for six power densities from 0.089 to 2.857 MW/kg ^{235}U . Burnup in these calculations is equal to the product of the fuel assembly specific power density and the

exposure time in days, times the constant $1.25\text{E-}3 \text{ kg}^{235}\text{U}$ burned per megawatt-day. At each burnup level, the fission product photon source was calculated in yearly increments through 20 years of fission product decay.

These photon source data as functions of ^{235}U burnup, assembly specific power density, and fission product decay time were then introduced into an MCNP model. The Monte Carlo model was used to calculate the photon flux in select regions around the fuel assembly. The photon source in all cases was uniformly distributed in the fuel meat of all fuel plates in a fuel assembly.

Based upon the calculated photon flux per unit photon source, the dose rates in rem/h were then calculated using the American National Standard (ANS) fluence-to-dose factors.

Based upon the dose rate calculated, these data for spent fuel assembly are usually known or can be reasonably estimated. The number of years that a spent fuel assembly will be self-protecting is directly linked to ^{235}U burn-up as a function of fission product decay time.

The objective of this research was to estimate the length of time that the spent fuel will be self-protecting that is having a dose rate greater than 100 rem/hr at 1m in air [23].

2.2.2 Mass Inventory of Spent Fuel of Research Reactors

The mass of uranium and transuranic elements in spent research reactor fuel must be specified. These data are, however, not always known or readily determined. The degree of physical protection given to spent fuel assemblies is largely dependent upon the photon dose rate of the spent fuel material. These dose rates were also not always known

or readily determined. It is important to know the dose rate of spent fuel assemblies at all time.

The mass inventory of the heavy metals in research reactor fuels has been calculated using the WIMS code. WIMS is a general purpose reactor physics program for core physics calculations.

It can provide simple pin cell calculations of reactivity to whole core estimates of power and flux distributions. The user can benefit from the flexibility of using predefined calculation routes or providing customized methods of solution using diffusion theory, discrete-ordinates, collision probability, characteristics or Monte Carlo methods. Models of each fuel assembly type were neutronicly burnt for a length of time corresponding to typical fuel-cycle lengths and U-235 burnup.

The dose rate was imported from Pond et al [23] where MCNP was used for the dose rate calculations.

Procedures have been developed to estimate the nuclear mass inventory and the photon dose of spent research reactor fuel assemblies. The procedures provided reasonable estimates based upon known fuel assembly parameters [24].

This research work will employ the use of ORIGEN-S and MCNP 6 computational codes which will be described into details in the succeeding chapter

A coordinated research project for the conversion of GHARR-1 started in the year 2006 and studies were performed on neutronic, thermal hydraulic and numerical computations of both the HEU and the proposed LEU. China Institute of Atomic Energy, the

manufacturer of the GHARR-1HEU core has developed a LEU core of high-density, low-enrichment UO_2 fuel under the RERTR program. The fuel has a total density up to 10.6g/cm^3 compare to the current HEU density of 3.456g/cm^3 . Total core loading of U-235 is 1358g compare to current core loading of 998g . U-235 enrichment has been reduced from 90.2% to 13% .

This is because LEU fuel requires approximately 20% enrichment of U-235 to achieve the same reactivity as the HEU core. Although the HEU core has a nominal power of 30 kW , the nominal power of the LEU core will increase to 34 kW in order to meet the flux level of $1 \times 10^{12}\text{ n/cm}^2\cdot\text{s}$. [25]. This will be achieved because the macroscopic cross section for fission will increase as the flux and the volume of the core remains constant. The relationship between power and flux is represented below

$$P = \frac{\phi_{th} \sum_f V}{3.12 \times 10^{10} \frac{\text{fission}}{\text{watt} - \text{sec}}} \quad (2.1)$$

where P is the power, ϕ_{th} is the thermal neutron flux, V is the volume of the core and \sum_f is the macroscopic cross section for fission.

Table 2.1 gives a comparison between the HEU and the LEU.

Table 2.1: Comparison of Key Parameters for GHARR-1 HEU and LEU Cores

Key Parameters	HEU	LEU
Fuel Meat	U-Al ₄	UO ₂
U-235 Total Core Loading, g	~ 998	~ 1358
U-235 Enrichment, wt %	90.2	13
U-234 content, wt%	1.0	0.2
U-236 content, wt%	0.5	0.25
Density of Meat, g/cm ³	3.456	10.6
Meat Diameter, mm	4.3	4.3
Cladding Diameter, mm	5.5	5.5
Thickness of He Gap, mm	None	0.05
Cladding Material	Al-303-1	Zirc-4
Number of Fuel Rods	344	339
Material for Grid Plates	LT-21	Zirc-4
Top Shim Tray (not modeled)	LT-21	LT-21
Number of Dummy Elements	6	11
Material for Dummy Elements	Al-303-1	Zirc-4
Number of Tie Rods	4	4
Material for Tie Rods	Al-303-1	Zirc-4
Adjuster Guide Tubes	4	4

In the utilization of MNSR facilities, one very important parameter is the use of neutron fluxes. It might be noted that the neutron flux is very important in neutron activation analysis, production of radioisotopes and also in research and development. For neutron

activation analysis, a minimum of 10^9 n/cm² s neutron flux is required which falls within the range of a typical steady state neutron flux of a research reactor. (the range is 10^{11} to 10^{14} neutrons/cm²·s) [25]

2.3 Ghana Research Reactor-1 (GHARR-1)

Ghana Research Reactor-1 (GHARR-1) is a Miniature Neutron Source Reactor (MNSR). It is a commercial MNSR similar to the Canadian SLOWPOKE in design [26].

It is a 30 kW tank-in-pool reactor, producing a peak or maximum thermal neutron flux in the core and its inner irradiation channels of 1×10^{12} n cm² s. The reactor which is designed to be compact and safe has made valuable contribution in the nuclear power industry. It is used mainly for Research and Development in reactor and nuclear engineering, neutron activation analysis, production of short-lived radioisotopes, human resource development for Ghana's nuclear program and for education and training.

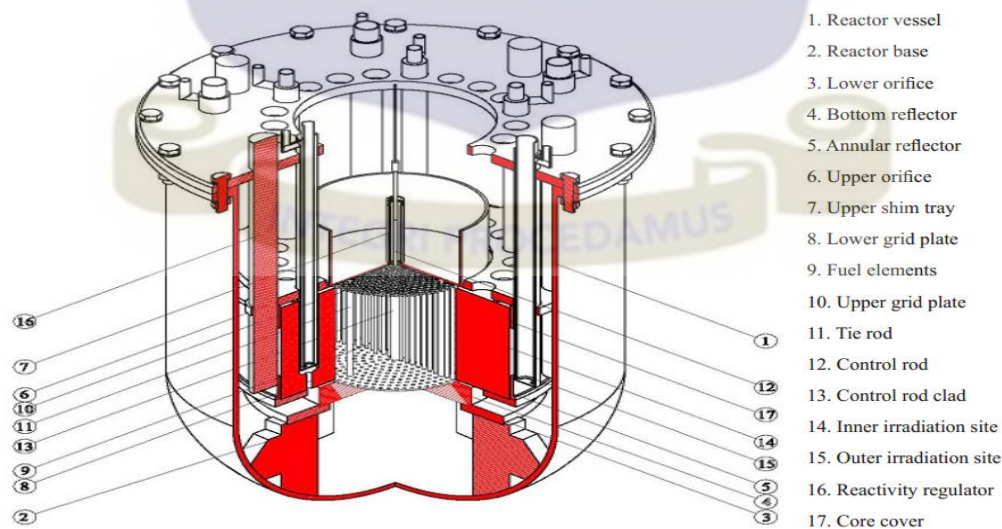


Fig. 2.13: The MNSR Research Reactor

[27]

GHARR-1 core employs 90.2% enriched uranium–aluminium alloy admixed in aluminium matrix as fuel as described in the table above. The diameter of the fuel meat is 4.3 mm and the thickness of the aluminium cladding material is 0.6 mm. The total length of the element is 248 mm. It is cooled by natural convection and moderated with light water.

The percentage of uranium in the U–Al dispersed in aluminium is 27.5% and the loading of U-235 in the core with 344 fuel elements is 990.72 g. In order to reduce the thermal resistance between fuel pellet and the cladding tube, the cladding is drawn to obtain mechanical close attachment between the cladding and the fuel meat.

The clearance between pellet and end plug is 0.5 mm, which is allowed for thermal expansion of the pellets. To ensure fuel element stability in the core, the lower end of the fuel rod is designed to have a tapered structure which enables a self-lock fit between the fuel end and the lower grid plate and thus the fuel rods and dummy elements are tightly locked to the lower grid plate while its upper end is free in the lattice of the upper grid plate.

The fuel cage consisting of 344 fuel pins, four tie and six dummy rods are concentrically arranged in 10 rings is located on a 50 mm thick bottom beryllium reflector of diameter 290 mm and is surrounded by a 100 mm thick metallic beryllium of height 238.5 mm.

The core is provided with a guide tube in the centre through which a central cadmium control rod with stainless steel clad moves to cover the full distance of the core of active height of 230 mm. The range of motion of the control rod is thus 0–230 mm. The bottom beryllium plate and the side beryllium annular form the inlet orifice and the supporting plate and the side beryllium annular form the outlet orifice. On top of the core is located

an aluminium shim tray provided for housing beryllium reflector shims of regulated thickness required for adjusting or compensating the core excess reactivity due to fuel depletion and samarium poisoning.

The regulated thickness refers to the required thickness of the reflector to compensate for reactivity loss due to fuel burn up and fission poisoning. The single control rod is used for regulation of power, compensation of reactivity and for reactor shutdown during normal and abnormal operations. The reactor core is located in the lower section of a sealed aluminium alloy vessel of diameter 0.6 m which is hanged on a frame across a stainless steel lined water pool of diameter 2.7 m and depth 6.5 m.

Presently, GHARR-1's core consists of a fuel assembly HEU (UAl_4 alloyed) fuel elements arranged in ten concentric rings about a central control rod guide tube, which houses the reactor's only control rod. The control rod's reactivity worth is about 7mk, providing a core shutdown margin of 3 mk of reactivity. The small core has a low critical mass. However, its relatively large negative temperature coefficient of reactivity is capable of boosting its inherent safety properties.

The small size of the core facilitates neutron leakage and escape in both axial and radial directions. To minimize such losses and thereby conserve neutron economy, the core is heavily reflected, respectively, on the side and underneath the fuel cage by a thick annulus and slab of beryllium alloy material. [26]

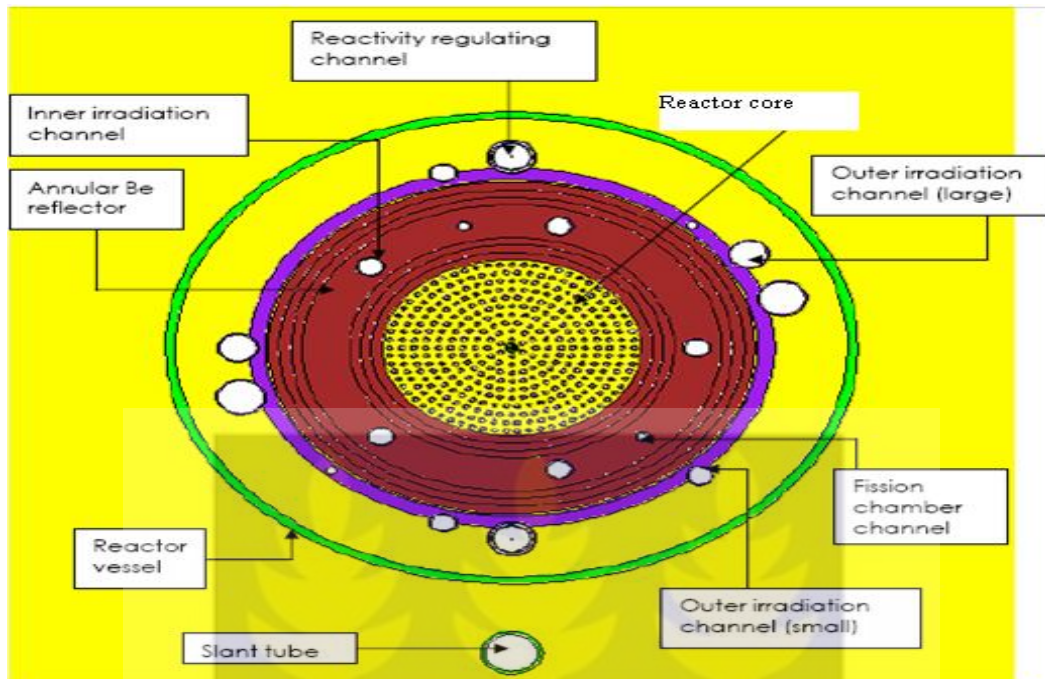


Fig 2.14: MCNP plot of the core configuration and associated experimental channels

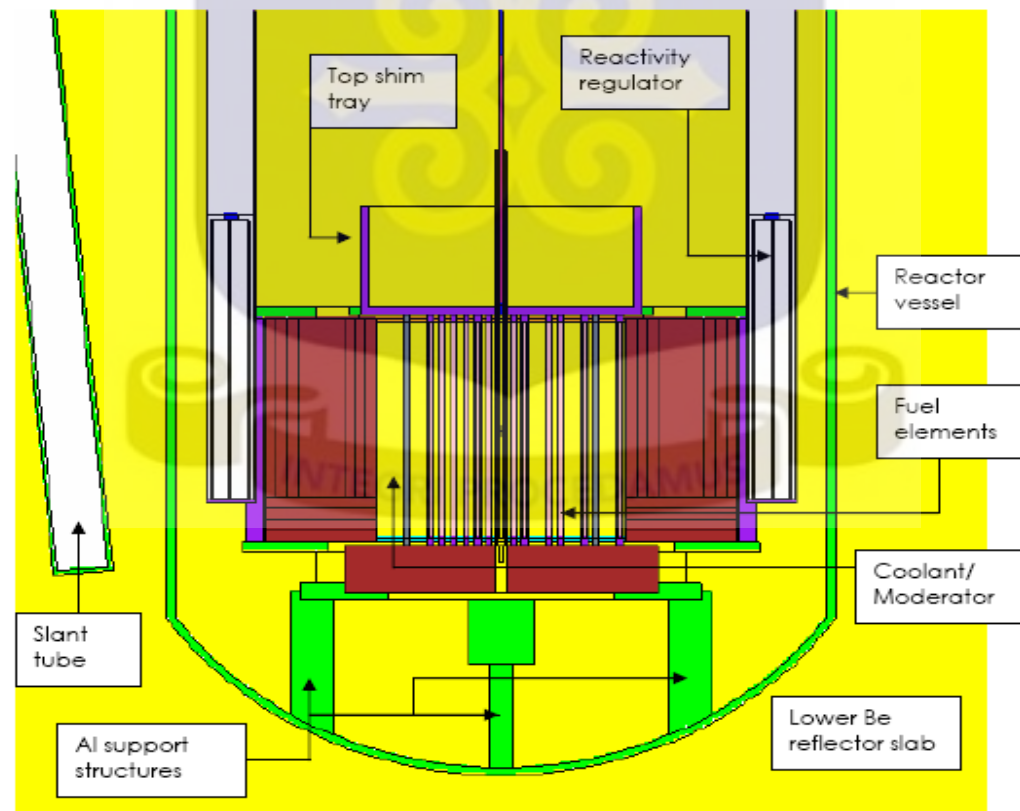


Fig 2.15: MCNP plot of vertical cross-section of GHARR-1 reactor (in full power mode)

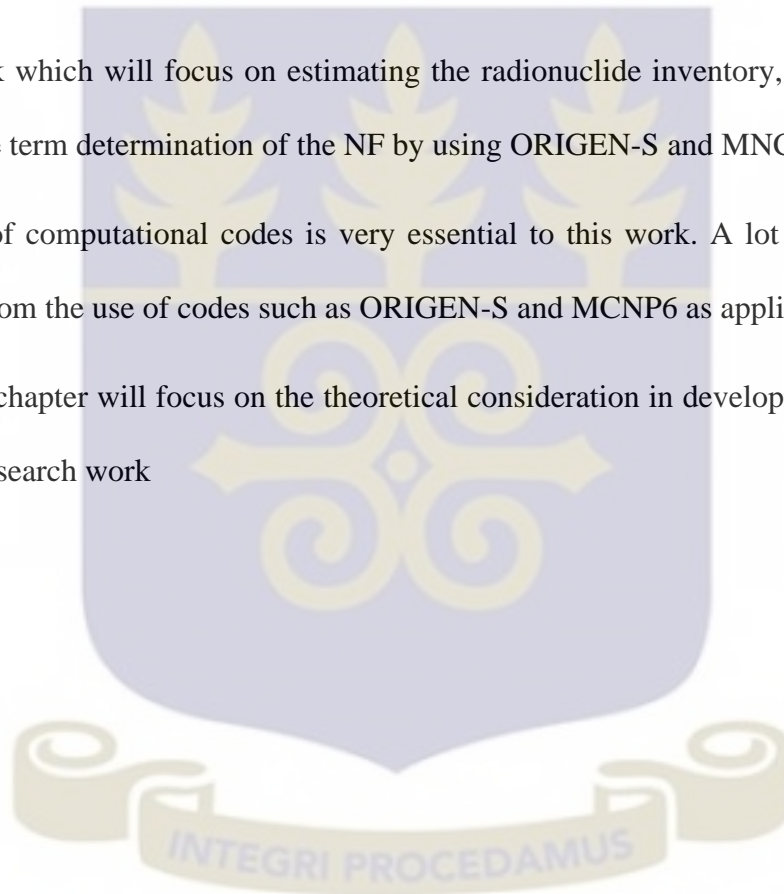
Various computational codes have been used for feasibility studies for core conversion program of GHARR-1. Some of the codes used were MCNP5 code for the neutronics studies, The REBUS code for the burnup, PARET code for the thermal hydraulic transient and the PLATE computational code for the study state analysis.

The studies done preceding this shows that it's very feasible to convert the HEU fuel to LEU fuel without any significant change to the reactor vessel

This work which will focus on estimating the radionuclide inventory, the criticality and the source term determination of the NF by using ORIGEN-S and MNCP6 codes

The use of computational codes is very essential to this work. A lot of advantages are derived from the use of codes such as ORIGEN-S and MCNP6 as applied in this study.

The next chapter will focus on the theoretical consideration in developing the codes used for this research work



CHAPTER THREE

3 THEORY

In the estimation of the radiation dose from the Spent Nuclear Fuel the behavior of the neutrons and photons and its associated criticality is made. In determining of the source term, the core inventory and radiation dose of Spent Nuclear Fuel (SNF) of GHARR-1, two computational codes were employed. The core inventory (the composition of the core made of fission fragments, actinides and activation products) and source term (the amount and isotopic composition of materials released or assumed to be released from a facility over a period of time) will be evaluated using ORIGEN-S code and the radiation dose as well as the criticality will be determined using MCNP6 code.

The theoretical considerations behind these codes are explained in this chapter.

3.0 ORIGEN-S

ORIGEN (Oak Ridge Isotope Generation code) applies a matrix exponential expansion model to calculate time-dependent concentrations, activities, and radiation source terms for a large number of isotopes simultaneously generated or depleted by neutron transmutation, fission, and radioactive decay. ORIGEN has been developed and maintained as the depletion and decay module in the SCALE code system. This version, ORIGEN-S, maintains the capability of other versions to be used as a standalone code but has the added ability to utilize multi-energy-group cross sections processed from standard ENDF/B evaluations. Within SCALE, transport codes can be used to model user-defined systems and calculate problem-dependent neutron-spectrum-

weighted cross sections that are representative of conditions within any given reactor or fuel assembly, and convert these cross sections into a library that can be used by ORIGEN-S. Time-dependent cross-section libraries may be produced that reflect fuel composition variations during irradiation.

The ORIGEN series of codes are widely used throughout the world for predicting the characteristics of SNF.

The original ORIGEN code released in 1973 was intended principally for the generic investigation of fuel cycle operations over a wide range of fuel design parameters. In 1982, the ORIGEN-S code was developed to interface with the neutronic modules of SCALE [27]

In determining the time dependence of nuclide concentrations, ORIGEN-S, solves for the formation and disappearance of a nuclide by radioactive disintegration and neutron transmutation. Mathematically,

$$\frac{dN_i}{dt} = \text{Formation Rate} - \text{Destruction Rate} - \text{Decay Rate} \quad (3.1)$$

The time rate of change of the concentration for a particular nuclide, N_i , in terms of these production and removal processes can be written as

$$\frac{dN_i}{dt} = \sum_{j=1}^m l_{ij} \lambda_j N_j + \Phi \sum_{k=2}^m f_{ik} \sigma_k N_k - (\lambda_i + \Phi \sigma_i) N_i \quad (i = 1, 2, \dots, m) \quad (3.2)$$

where

N_i = atom density of nuclide i ,

λ_i = radioactive disintegration constant of nuclide i ,

- σ_i = spectrum-averaged neutron absorption cross section of nuclide i,
- Φ = space- and energy-averaged neutron flux,
- l_{ij} = branching fractions of radioactive disintegrations from other nuclides j,
- f_{ik} = branching fractions for neutron absorption by other nuclides k that lead to the formation of species i.

The equation (3.2) is written for a homogeneous medium containing a space and energy-averaged neutron flux, Φ , with one-group, flux-weighted average cross sections, σ_i , representing the reaction probabilities.

The mathematical treatment in ORIGEN-S assumes that the space-energy-averaged flux can be considered constant over a sufficiently small time interval, Δt . Similarly, it is assumed that a single set of flux-weighted neutron cross sections can be used over the same time step. For a given time step, these assumptions are necessary if equation (3.2) is to be treated as a first-order, linear differential equation. The time-dependent changes in the flux and weighted cross sections are simulated in ORIGEN-S by providing a capability of updating the values for the space-energy-averaged flux and, therefore, for the weighted cross sections for each successive time step, Δt_k , Δt_{k+1} , ..., Δt_n . These values are updated based on data provided by the neutron transport solver in SCALE [29].

3.0.1 SOLUTION WITH THE MATRIX EXPONENTIAL METHOD

ORIGEN-S analytical model described by Equation (3.2) represents a coupled set of linear, homogeneous, first-order differential equations with constant coefficients. Equation (3.2) can be thus written in matrix notation as

$$\vec{N} = AN \quad (3.3)$$

where N is a vector of nuclide concentrations and A is the transition matrix containing the rate coefficients for nuclide production and destruction by decay and neutron transmutation. Equation (3.3) has

$$N = \exp(At)N(0) \quad (3.4)$$

as its solution where $N(0)$ is a vector of initial nuclide concentrations.

Equivalent to a series expansion for the exponential function, the matrix exponential function, $\exp(At)$ in equation (3.4), can be written as

$$\exp(At) = I + At + \frac{(At)^2}{2!} + \dots = \sum_{m=0}^{\infty} \frac{(At)^m}{m!} \quad (3.5)$$

with I being the unit matrix. Equations (3.4) and (3.5) describe the matrix exponential method, which yields a complete solution to the problem. However, in certain instances related to limitation in computer precision, difficulties occur in generating accurate values of the matrix exponential function, thus, alternative procedures using either the generalized Bateman equations or Gauss-Seidel iterative techniques are applied. [29].

A straightforward solution of equation (3.4) through the expansion in equation (3.5) would require the storage of the complete transition matrix. A recursion relation has been developed to avoid excessive memory storage requirements. Substituting for the matrix exponential function in Equation (3.4), we have

$$N = \left[1 + At + \frac{(At)^2}{2!} + \frac{(At)^3}{3!} + \dots \right] N(0) \quad (3.6)$$

The recursion relation may be observed by considering the solution of Equation (3.6) for a particular nuclide, N_i . The result is a series of terms that arise from the successive post-multiplication of the transition matrix by the vector of nuclide concentration increments produced from the computation of the previous terms. Within the accuracy of the series expansion approximation, physical values of the nuclide concentrations are obtained by summing a converged series of these vector terms. The elements of the transition matrix, a_{ij} , are the first-order rate constants for the formation of nuclides i from nuclides j . The solution in terms of these rate constants is written as

$$N_i = N_i(0) + t \sum_j a_{ij} N_j(0) + \frac{t}{2} \sum_k [a_{ik} t \sum_j a_{kj} N_j(0)] + \frac{t}{3} \sum_m \{ a_{im} \times \frac{t}{2} \sum_k [a_{ik} t \sum_j a_{kj} N_j(0)] \} + \dots \quad (3.7)$$

where the range of indices, j, k, m , is 1 to M for a $M \times M$ matrix A

The recursion relation is developed from Equation (3.7) by defining the terms c_i^n

$$c_i^0 \equiv N_i(0), c_i^{n+1}$$

$$c_1^0 = \frac{t}{n+1} \sum_j a_{ij} c_j^n \quad (3.8)$$

The solution for N_i will become

$$N_i = \sum_{n=0}^{\infty} c_i^n \quad (3.9)$$

Equation (3.9) can be used in obtaining the solution for a system of nuclides given in equation (3.4) requires the storage of only two vectors, C^n and C^{n+1} , in addition to the current value of the solution [29].

Various tests are conducted in ORIGEN-S to ensure that the summations indicated in equation (3.9) do not lose accuracy owing to relative magnitudes or small differences between positive and negative rate constants. Nuclides with large rate constants are removed from the transition matrix and treated separately. For example, in the decay chain $A \rightarrow B \rightarrow C$, if the decay constant for B is large, a new rate constant is inserted in the matrix for $A \rightarrow C$. This technique was originally employed by Ball and Adams [30].

The determination of which transitions are to be reduced from the matrix involves the calculation of the matrix norm. The norm of the matrix A is defined by Lapidus and Luus [26] as being the smaller of the maximum-row absolute sum and the maximum-column absolute sum. That is, the norm, $[A]$, is given by

$$[A] = \min \left\{ \max_i \sum_j a_{ij}, \max_j \sum_i a_{ij} \right\} \quad (3.10)$$

In order to maintain precision in performing the summations of equation (3.9), the matrix norm is used to balance the user-specified time step, t , with the precision associated with the word length employed in the machine calculation. Lapidus and Luus have shown that the maximum term in the summation for any element in the matrix exponential function cannot exceed $([A]t)^n/n!$, where n is the largest integer not larger than $[A]t$. In the ORIGEN-S program, $[A]t$ is restricted by

$$[A]t \leq -2\ln(0.001) = 13.8155 \quad (3.11)$$

This value restricts the size of the maximum term to approximately 10^5 . Current computer operating systems (i.e., those using the 32-bit word size) typically retain 16 significant decimal figures when performing double-precision arithmetic. Given the maximum term of 10^5 and 16 significant-figure precision, ORIGEN-S can maintain five significant-figure accuracy in values as small as 10^{-6} . The precision of the calculations on any computers can be easily determined for any particular machine precision, and this procedure has been automated in ORIGEN-S.

The restriction described by equation (3.11) is maintained by removing nuclides from the transition matrix when $e^{-dt} < 0.001$, where $-d$ is the diagonal element for the nuclide. Since d is the sum of decay constant plus the product of total absorption cross section and flux, the sum of the absolute values in the column containing d cannot exceed $2d$. It always equals $2d$ when all of its daughter nuclides are contained in the matrix (i.e., its loss rate equals its product transition rate). Even though the sum of the absolute values in the row containing d may exceed $2d$, the norm $[A]$ defined by equation (3.10) never exceeds twice the maximum value of d in the reduced matrix. Thus,

$$[A]t \leq 2dt = -2\ln(e^{-dt}) \leq -2\ln(0.001) \quad (3.12)$$

Note that nuclides are considered short-lived if their effective half-lives are less than about 10% of the time interval ($1/210 = 1/1024 = 0.001$).

A generalized equation may be derived for computing the maximum norm of A_t , given m , the number of significant figures of the computer word for a specified machine, and j , the required number of significant figures in all results. It is preferred to cast the equation in terms of the maximum absolute diagonal element, $|d|_t$, where $[A] = |2|$ holds true for any A constructed by ORIGEN-S.

In ORIGEN-S, all nuclides for which $\exp(-|dt|) < 0.001$ are removed from A and must be handled by alternative procedures. Increasing this restriction value to 0.12, or 0.05, would result in more computer time and possibly other problems [29].

The matrix norm is also used in the determination of the number of expansion terms required for convergence of the series in equation (3.9). The number of expansion terms is set to $7/2 [A]t + 6$, sufficient to limit the summation error to less than 0.1% in most applications. For example, for $[A]t$ equal to 13.8155, the summation will be performed using 54 terms. The minimum number of terms used in the expansion is 21.

In applications where the nuclides of interest are in long transmutation chains, the above algorithm may not yield accurate concentrations for those nuclides near the end of the chain that are significantly affected by those near the beginning of the chain. For this reason, the algorithm in ORIGEN-S allows the user to set the number of expansion terms. As guidance in determining an appropriate value for these applications, given

nuclides with atomic number (Z) and mass (A) on the extremities of the chain of interest, $Z_1A_1 \rightarrow Z_2A_2$, the expression below will estimate the number of terms required to calculate the concentration of Z_2A_2 .

$$n = |Z_1 - Z_2| + |A_1 - A_2| + 5 \quad (3.13) \quad [29] [30] [31]$$

3.0.2 SOLUTION TO THE NUCLIDE CHAIN EQUATIONS

This separation of nuclides due to the removal of nuclides with short half-lives from the transition matrix which are treated separately involves the solution of the nuclide chain equations.

In conjunction with maintaining the transition matrix norm below the prescribed level, a queue is formed of the short-lived precursors of each long-lived isotope. These queues extend back up the several chains to the last preceding long-lived precursor. The queues include all nuclides whose half-lives (loss due to decay and neutron absorption) are less than 10% of the time interval. A generalized form of the Bateman equations developed by Vondy [32] is used to solve for the concentrations of the short-lived nuclides at the end of the time step.

For an arbitrary forward-branching chain, Vondy's form of the Bateman solution is given by

$$N_i = N_i(0)e^{-d_it} + \sum_{k=1}^{i-1} N_k(0) \left[\sum_{j=k}^{i-1} \frac{e^{-d_jt} - e^{-d_it}}{(d_i - d_j)} a_{j+1,j} \prod_{\substack{n=k \\ n \neq j}}^{i-1} \frac{a_{n+1,n}}{d_n - d_j} \right] \quad (3.14)$$

where $N_i(0)$ is the initial concentration of the first precursor, $N_2(0)$ that of the second precursor, a_{ij} is the first-order rate constant and d_i is equal in magnitude to the diagonal element, or $d_i = -a_{ii}$. Bell has recast Vondy's form of the solution through multiplication and division by $\prod_{n=k}^{i-1} d_n$

Rearranging terms the obtains

$$N_i = N_i(0)e^{-d_i t} + \sum_{k=1}^{i-1} N_k(0) \prod_{n=k}^{i-1} \frac{a_{n+1,n}}{d_n} \left[\sum_{j=k}^{i-1} \frac{e^{-d_j t} - e^{-d_i t}}{(d_i - d_j)} \prod_{\substack{n=k \\ n \neq j}}^{i-1} \frac{d_n}{d_n - d_j} \right] \quad (3.15)$$

The first product over isotopes n is the fraction of atoms that remains after the k_{th} particular sequence of decays and captures. If this product falls less than 10^{-6} the contribution of this sequence to the concentration of nuclide i is neglected. Indeterminate forms arising when $d_i = d_j$ or $d_n = d_j$ are evaluated using L'Hôpital's rule. These forms occur when two isotopes in a chain have the same diagonal element.

The solution given by equation (3.15) is applied to calculate all contributions to the queue end-of-interval concentrations of each short-lived nuclide from initial concentrations of all others in the queue described above. Also, equation (3.15) is applied to calculate the contributions from the initial concentrations of all short-lived nuclides in the queue to the long-lived nuclide that follows the queue in addition to the total contribution to its daughter products. These values are appropriately applied in the program, either before or after the matrix expansion calculation is performed, to make the concentration of the long-lived nuclide or the total of its daughters the correctly computed quantity.

Equation (3.15) is applied in making adjustments to certain elements of the final transition matrix, which now excludes the short-lived nuclides. The value of the element must be determined for the new transition between the long-lived precursor and the long-lived daughter of a short-lived queue. The element is adjusted such that the end-of-interval concentration of the long-lived daughter calculated from the single link between the two long-lived nuclides (using the new element) is the same as what would be determined from the chain including all short-lived nuclides. The method assumes zero concentrations for precursors to the long-lived precursor. The computed values asymptotically approach the correct value with time as successive time intervals are executed. (For this reason, at least five to ten time intervals during the decay of discharged fuel are reasonable, because long-lived nuclides have built up by that time).

In the instance that a short-lived nuclide has a long-lived precursor, an additional solution is required. First, the amount of short-lived nuclide i due to the decay of the initial concentration of long-lived precursor j is calculated as

$$N(t)_{j \rightarrow i} = N_j(0) a_{ij} \frac{e^{-a_{ij}t}}{a_{ii} - a_{ij}} \quad (3.16)$$

from equation (3.15) with $a_{kk} = d_k$ and assuming $\exp(-d_{it}) \ll \exp(-d_{jt})$. However, the total amount of nuclide i produced depends upon the contribution from the precursors of precursor j , in addition to that given by equation (3.16). The quantity of nuclide j not accounted for in equation (3.16) is denoted by $N'_j(t)$, the end-of-interval concentration minus the amount that would have remained had there been no precursors to nuclide j ,

$$N_j'(t) = N_j(t) - N_j(0)e^{-a_{jj}t} \quad (3.17)$$

Then the short-lived daughter and subsequent short-lived progeny are assumed to be in secular equilibrium with their parents, which implies that the time derivative in equation (3.17) is zero.

$$N = 0 = \sum_j a_{ij} N_j \quad (3.18)$$

The queue end-of-interval concentrations of all the short-lived nuclides following the long-lived precursor are augmented by amounts calculated with equation (3.18). The concentration of the long-lived precursor used in equation (3.16) is that given by equation (3.17). The set of linear algebraic equations given by equation (3.18) is solved by the Gauss-Seidel iterative technique. This algorithm involves an inversion of the diagonal terms and an iterated improvement of an estimate for N_i through the expression

$$N_i^{k+1} = -\frac{1}{a_{ii}} \sum_{j \neq i} a_{ij} N_j^k \quad (3.19)$$

Since short-lived isotopes are usually not their own precursors, this iteration often reduces to a direct solution. [29]

3.0.3 PHOTON SOURCES AND SPECTRA

The gamma-ray source strengths and energy spectra computed by ORIGEN-S include photons arising from X-rays, gamma-rays, bremsstrahlung, spontaneous fission gamma rays, and gamma rays accompanying (α,n) reactions. Photons from X-rays and gamma rays emitted from the nucleus for all decay modes are stored in the

gamma library as line-energy and intensity data. Continuum spectra from bremsstrahlung, spontaneous fission, and (α ,n) interactions are represented as binned pseudo-line data.

The ability of ORIGEN-S to apply line-energy data allows photon energy spectra to be calculated in any user-specified energy group structure directly. When the data from photon data libraries are converted to multigroup yields by ORIGEN-S, the intensities of the photons are adjusted to conserve energy of the spectrum. The adjusted group intensity is given by

$$I_g = I_a \left(\frac{E_a}{E_g} \right) \quad (3.20)$$

where I_a = actual photon intensity from the gamma library (photons per disintegration),

E_a = actual photon energy (MeV),

E_g = mean energy of the group (MeV),

I_g = group photon intensity (photons per disintegration).

If the actual photon energy E_a is near a group boundary, the group intensity may be split between two groups. To determine when this split occurs, a factor f is computed as

$$f = \frac{E_a - E_l}{E_u - E_l} \quad (3.21)$$

where E_l = lower energy bound of the group and E_u = upper energy bound of the group (MeV).

If $f \leq 0.03$, the intensity I_g is split equally between group g and the next lower energy group, unless group g is the lowest group. If $f \geq 0.97$, the intensity I is split equally between group g and the next higher energy group, unless group g is the highest group. If $0.03 < f < 0.97$, the intensity I_g is not split between adjacent groups.

If a nuclide decays by gamma emission but does not have evaluated spectral data in the photon library, the recoverable gamma energy determined from the ENDF/B decay evaluations is saved and the extra energy is accounted for by renormalizing the spectra [29].

3.0.4 TIME DEPENDENCE OF THE NEUTRON FLUX

There is the option of specifying either a fixed value for the neutron flux or the specified power of the system. If the power is used, the neutron flux is determined from the specific power, microscopic reaction cross sections, the recoverable energy released for each reaction, and the fissionable and absorbing nuclide concentrations at any point in time. The thermal power due to neutron irradiation is given as

$$P = 1.6 \times 10^{-19} \sum_{ij} Q_{ij} N_{ij} \sigma_{ij} \phi \quad (3.22)$$

where P is the specific power in MW, 1.6×10^{-19} MW equals 1 MeV/s, N_{ij} is the number of atoms for nuclide i , σ_{ij} is the reaction cross section for nuclides i and reaction types j (fission, radiative capture, etc.) in cm^2 , Q_{ij} is the recoverable energy in MeV released from fission and capture, and ϕ is the neutron flux in neutrons/ $(\text{cm}^2 \cdot \text{s})$.

For a specified constant power level, the flux as a function of time varies with the concentrations of the absorbing nuclides. Solving Equation (3.22) for flux, we write the flux as a function of time as, the expression becomes

$$\phi(t) = \frac{6.242 \times 10^{18} P}{\sum_{ij} N_i(t) \sigma_{ij} Q_{ij}} \quad (3.23)$$

where the variables are as denoted above

Values of the recoverable energy for fission and radioactive capture for 24 fissile isotopes and other important neutron-absorbing nuclides are based on ENDF/B data. An average value of 5 MeV for prompt energy release for radioactive neutron capture is applied for all other nuclides, which contribute usually less than 0.3% of the energy per fission. The energy carried off by neutrinos is not included in this value. The user has the option to specify a constant recoverable energy per fission value of 200 MeV/fission.

ORIGEN-S performs a flux-correction calculation to obtain an estimate of the average flux over the irradiation time interval, t . The start-of-interval flux is first calculated for the initial compositions. An explicit depletion calculation is then carried out using the initial flux to estimate the end-of-interval compositions. The flux is then recalculated as the average of the starting and ending interval flux, and a second depletion calculation is performed using the average interval flux. If the average flux differs from the value at the beginning of the time step by more than 20%, a warning is printed to use smaller time steps and execution will stop. The user must then reduce

the specified time step size to ensure an accurate estimate of the average flux over the interval [29]

3.1 MCNP6

MCNP is a general-purpose Monte Carlo N-Particle code that can be used for neutron, photon, electron, or coupled neutron/photon/electron transport, including the capability to calculate eigenvalues for critical systems. The code treats an arbitrary three-dimensional configuration of materials in geometric cells bounded by first-degree and second-degree surfaces and fourth-degree elliptical tori [33].

MCNP6 which is part of the MCNP family is a general-purpose, continuous-energy, generalized-geometry, time dependent, Monte Carlo radiation-transport code designed to track many particle types over broad ranges of energies. MCNP6 represents the culmination of a multi-year effort to merge the MCNP5 and MCNPX codes into a single product comprising all features of both. It has been expanded to contain new tally, source, and variance-reduction options are available to the user as well as an improved plotting capability. The capability to calculate keff eigenvalues for fissile systems remains a standard feature. This initial production release of MCNP6 contains 16 new features not previously found in either code. These new features include the abilities to import unstructured mesh geometries from the finite element, to transport photons down to 1.0eV, to model complete atomic relaxation emissions, and to generate or read mesh geometries for use with the LANL discrete ordinates from other codes to mention just a few [34].

The behavior of individual neutrons and nuclei cannot be predicted but the average behavior of a large population of neutrons can be described quite accurately if we have knowledge of neutron fluxes, cross-sections, and reaction rates. Solving particle transport problems with the Monte Carlo method is quite simple and can be done in two basic ways which are the mathematical method for numerical integration and computer simulation for physical processes. Mathematical approach is useful for importance sampling, convergence, variance reduction, random sampling technique and eigenvalue calculation scheme whilst the simulation approach is useful for collision physics tracking, tallying and so on.

Monte Carlo methods solve integral problems (that is the integral form of Boltzmann equation). Most theory on Monte Carlo deals with fixed source problems. Eigenvalue problems are needed for criticality and reactor physics calculation. The key to Monte Carlo methods is the notion of random sampling. When Monte Carlo is used to solve integral Boltzmann transport equation, it models the outcome of physical events (example neutron collision, fission process, source etc). The computational geometry models the arrangement of materials [35].

The time dependent linear Boltzmann transport equation

$$\Psi(r, v) = \int \left[\int \Psi(r', v') C(v' \rightarrow v, r) dv' + Q(r', v) \right] T(r' \rightarrow r, v) dv' \quad (3.24)$$

where $\Psi(r, v)$ = particle collision density

$Q(r', v)$ = source term

$C(v' \rightarrow v, r')$ = collision kernel, change velocity at fixed position r'

$C(r' \rightarrow r, v)$ = transport kernel, change in position r at a fixed velocity v

$$\text{Angular Flux} = \Psi(r, v) = \frac{\Psi(r, v)}{\Sigma(r, |v|)}$$

$$\text{Scalar Flux} = \phi(r, |v|) = \int_{\bar{\Omega}} \frac{\Psi(r, v)}{\Sigma(r, |v|)} d\bar{\Omega}, \quad \text{where, } v = |v|\bar{\Omega}$$

$$\text{Solid Angle} = d\bar{\Omega}$$

Source term for the Boltzmann equation

$$Q(r, v) = \left\{ \begin{array}{l} S(r, v) \\ S(r, v) + \int \Psi(r, v') F(v' \rightarrow v, r) dv' \\ \frac{1}{\kappa} \int \Psi(r, v') F(v' \rightarrow v, r) dv' \end{array} \right\} \quad (3.25)$$

where

$S(r, v)$ = Fixed source term

$F(v' \rightarrow v, r)$ = creation operator (due to fission), particles at (r, v') creates particles at (r, v)

κ = eigenvalues

[35][36]

3.1.0 PARTICLE TRACKS

When a particle starts out from a source, a particle track is created. If that track is split 2 for 1 at a splitting surface or collision, a second track is created and there are now two tracks from the original source particle, each with half the single track weight. If one of the tracks has an $(n, 2n)$ reaction, one more track is started for a total of three. A track refers to each component of a source particle during its history. Track length tallies use

the length of a track in a given cell to determine a quantity of interest, such as fluence, flux, or energy deposition. Tracks crossing surfaces are used to calculate fluence, flux, or pulse-height energy deposition (surface estimators). Tracks undergoing collisions are used to calculate multiplication and criticality (collision estimators). Within a given cell of fixed composition, the method of sampling a collision along the track is determined using the following theory. The probability of a first collision for a particle between l and $l+dl$ along its line of movement is given by

$$p(l) dl = e^{-\sum_t l} \sum_t dl \quad (3.26)$$

where \sum_t is the macroscopic total cross section of the medium and is interpreted as the probability per unit length of a collision. Setting ξ the random number on $[0,1)$, to be we obtain the expression below

$$\xi = \int_0^l e^{-\sum_t s} \sum_t ds$$

$$\xi = 1 - e^{-\sum_t l} \quad (3.27)$$

Hence it follows that the length, l , becomes

$$l = -\frac{1}{\sum_t} \ln(1 - \xi) \quad (3.28)$$

But, because $1 - \xi$ is distributed in the same manner as ξ and hence may be replaced by ξ , we obtain the well-known expression for the distance to collision,

$$l = -\frac{1}{\sum_i} \ln(\xi) \quad (3.29)$$

3.1.2 CRITICALITY CALCULATIONS

The ability to sustain a chain reaction by the fission of neutrons is characterized by k_{eff} the eigenvalue to the neutron transport equation. Criticality, k_{eff} is thought of as the ratio between the numbers of neutrons in successive generations, with the fission process regarded as the birth event that separates two generations of neutrons. [37]

A system is said to be critical when k_{eff} is equal to 1 that's to say the chain reaction will self sustaining. For subcritical systems, k_{eff} will be less than 1 in this case, the chain reaction will not sustain itself. The system is said to be supercritical when k_{eff} is greater than 1, thus the number of fissions in the chain reaction will increase with time. In addition to the geometry description and material cards, all that is required to run a criticality problem is a KCODE card and an initial spatial distribution of fission points using the KSRC card, the SDEF card, or an SRCTP file.

Calculating k_{eff} consists of estimating the mean number of fission neutrons produced in one generation per fission neutron started. A generation is the life of a neutron from birth in fission to death by escape, parasitic capture, or absorption leading to another fission process.

In MCNP, the computational equivalent of a fission generation is a k_{eff} cycle, that is, a cycle is a computed estimate of an actual fission generation. Processes such as (n,2n) and (n,3n) are considered internal to a cycle and do not act as termination because, the

fissioned neutrons acts as source for the beginning of a new fission chain reaction [1][2][34].

These codes were used to estimate the source term, determine the core inventory and ascertain the criticality of the NF as well as estimate the dose rate emanating from the NF of GHARR-1. Several processes and procedures were used to obtain these results.

The ensuing chapter outlines the various methods employed in arriving at these results.



CHAPTER FOUR

4 METHODOLOGY

Two computational codes were used to determine the radiation dose rate of GHARR-1's spent nuclear fuel. ORIGEN-S was used to compute the radionuclide inventory and source term whilst MCNP6 was used to calculate criticality and dose rate.

4.0 ORIGEN-S

ORIGEN-S is a time-dependent point-depletion code which is used to estimate source term and nuclide concentrations of large number of isotopes. The depletion is by radioactive decay, fission or transmutation. It is widely used in nuclear reactor and processing plant for design studies, studies for spent fuel transportation and storage, fuel inventory, fuel burnup, decay heat, radiation safety analyses, and environmental assessments. The matrix exponential expansion model is used in ORIGEN-S.

The code solves the transmutation equations using libraries of radioactive decay data and 1-group cross section data. The base code libraries allow the tracking of over 100 actinides and nearly 900 fission product nuclides. Pre-calculated libraries of 1-group cross section data are available for use in ORIGEN-S for several reactor systems. A standard library for an oxide-fueled LWR, the so-called bwrus library, represents the closest potential match to the basic neutronics characteristics of the MNSR core. It is preferable to replace cross section data for some or all of the nuclides in the library with data that are more appropriate for the particular system under analysis. Replacement cross section data were calculated for only a dozen also selected actinides and fission

products. The calculated 1-group capture and fission cross sections at the mid-core life. ORIGEN-S code tracks radioactive nuclide inventories for three groups according to their production route. These groups are activation products, actinides and daughters, and fission products. Some nuclides may appear in more than one group. The radioactive nuclide activities (in curies) are produced both during the irradiation period and cooling period afterward. A large amount of nuclide inventory data is available for analysis.

4.0.1 Determination of source term and isotopic inventory

The ORIGEN-S input deck was set up in order to determine the source term that was used in the MCNP6 input deck to help determine the dose rate emanating from the SNF. The ORIGEN deck is divided into blocks (each block contains important information that helps in depleting the core). The core depletion takes into consideration the composition of decay nuclides and fission products as well as light elements as a result of burnup. Key parts of the input deck include the nuclide identity, composition of nuclide, and the results desirable as well as specific neutron and gamma energies desirable (that is all these pieces of information are vital and used to set up the input deck). The nuclide composition and continuous nuclide feed rate were specified for nuclides of interest. The cut off fraction was overridden to give way for output summary table. Two vectors were set up in the deck and nuclide concentration data in one vector were moved into the other vector depending on the calculation of interest. The decay and cross section libraries were specified so that the code works with those selected data. The code was instructed to control the printing of only relevant input data libraries. The deck was also set up to track photon production rate in 39 energy groups. Since the code was written for nuclear power plants, the code was instructed to read nuclide identifiers for

replacement decay and cross section data cards in order to suit the MNSR. The average burnup, flux and specific power for an irradiation was calculated. Neutron flux and power were specified for irradiation of a single interval. Decay of a single interval was also specified. The table type to be printed (element, nuclides or summary) was specified for actinides, light elements and fission products. The power history of GHARR-1 used was 15kW. It was assumed to operate for four hours a day, four days a week, four weeks a month and eleven months in a year. A cumulative number of operating days was used. The decay time in steps of ten was used in order to monitor the short lived radionuclides. The average of running power especially the historic operation was determined and used. Near the end of life of the fuel, finer detail depletion is desirable but the historic operation would have lost its entire short lived isotope; hence coarse detail depletion is more convenient (20years, 10 months, 10 weeks, 1 week and the last five days to the core removal). The flux spectrum of the reactor which is obtained from an initial run of the MCNP is used. The flux spectrum in the MCNP output has many groups as defined in the corresponding MCNP flux tally in the input deck. COUPLE has cross section libraries for the different nuclides and reactions arranged by energy groups. Available libraries have 44, 49, 200 or 238 groups. The most accurate or finely partitioned library (238groups) according to the energy spectrum was used. This should provide more than enough precision for most practical purposes [38].

The alternative, as it happened with ORIGEN2, which didn't use COUPLE in Abrefah et al, 2014 was to select a single effective cross section value according to a typical flux energy profile (thermal, PWR, BWR, SFR, ...), [39] which may not accurately correspond to that in my reactor, or ask MCNP to estimate the cross section of each

isotope and reaction of interest based on the reaction rate obtained in the corresponding MCNP run. It is far more convenient to ask MCNP for the neutron flux in each energy group (238 in total) and allow COUPLE to quickly calculate the effective cross section for any reaction that might be needed for the ORIGEN-S calculations.

After the reactor with the HEU core is shut down for conversion, there is a waiting period intended to reduce the activity of the irradiated fuel and its decay heat by letting the shorter-lived isotopes to decay. This reduces the shielding requirements during core removal and simplifies the operation, while also reducing the heat load on the transport canister, though the latter is probably less of an issue in this study. A reasonable waiting time might be one month, after that the rate of activity decrease may be relatively slow, so the benefit of waiting more after that time may not overcome the drawback of further delaying the conversion and the normal operation of the reactor. It is basically an arbitrary choice, and possibly a conservative one, since one month is likely the minimum time period expected between shut down and conversion.

4.1 MCNP

MCNP is a three-dimensional transport theory code that solves complex time-dependent problem by simulation of the particle transport history. It takes into consideration the geometry description and continuous energy cross section to simulate time dependent transport processes [32][40]. The transport theory method is used to simulate the transport and interaction of particles because of the material complexity. Basically, there are two methods of solution to the transport equation, which are the deterministic method

and the Monte-Carlo method [41]. The Monte-Carlo method can mimic the physical model accurately by using a unifying geometry and can perform particle transport based on continuous energy nuclear cross sections [38]. It solves the integral transport equation and is expensive with computer time (the code takes a long time to run the code).

4.1.0 GHARR-1 MCNP model

The model was developed using the Ghana MNSR as a reference MNSR facility. The MCNP6 transport code was used to perform the Monte Carlo calculations. Nuclear data for fissile and non-fissile isotopes associated with materials (fuel, fuel clad, coolant, moderator, control rod and clad, reflectors, structural components) of the physical model was chosen from ENDF/B-V I nuclear data libraries. Some nuclear data from LLNL, LANL were utilized. The special $S(\alpha,\beta)$ scattering feature was applied in the nuclear model to treat thermal scattering in beryllium and hydrogen in light water for the reflector material and water regions respectively of the GHARR-1 Monte Carlo model.

A7-subdivision structure of the Hansen–Roach continuous neutron energy group was used in the Monte Carlo model. Neutronic analyses were performed using a condensed 3-group neutron energy structure: up to 0.625eV for thermal neutrons, <8.21eV for epithermal neutrons and up to 20MeV for fast neutrons.

4.1.1 Analysis of GHARR-1 MCNP simulated results

Neutron transport simulations were run for 265,000,000 source particle histories (500,000 source particles and 530 KCODE cycles) with an initial criticality (k_{eff}) guess of 1.004. Fifty cycles were initially skipped before the actual runs. The unnormalized particle flux

tallies were then normalized to get the actual fluxes. To accomplish this, some parameters such as the neutron fission q-value, loss to fission ratio provided in the MCNP code were utilized to calculate the normalization factor as described in the MCNP manual and presented herein. The conversion factor below was used in the conversion.

$$\left(\frac{1J/s}{W}\right)\left(\frac{1MeV}{1.60205e^{-13}J}\right)\left(\frac{fissions}{180.88MeV}\right) = 3.450908E+10 fissions/Ws \quad (4.1)$$

The source strength of the reactor is calculated by the factor: $3.450908 \times 10^{10} P$ (W),

where P is the operating power of the reactor. For a steady state operation, the number of neutrons/fission $\bar{\nu}$ is approximately 2.4. The normalization factor for the unnormalized tallies was calculated by using the factor,

$$\frac{3.450908E+10P(W)\bar{\nu} * tally}{volume} \quad (4.2)$$

Where $\bar{\nu}$ is the number of neutrons /fission

4.1.2 Dose estimation using MCNP6

The input deck for the dose calculation is fundamentally similar to that of the criticality calculation. However, new additional information is required in the input deck to help calculate the dose rate. Cards such as d1, d2, d3, sp1, sp2, si2, si3 and so on were introduced. Values basically from the output of previous calculations, such as the radial and axial flux distribution provided by the corresponding tallies of MCNP neutronics calculations, or ORIGEN calculations in the case of d2.

Most of the information are extracted from the results and put into the new MCNP input deck for dose calculations.

SDEF (source definition) card was used to define the source. In this case, a uniform neutron source definition with a cylindrical shape is desired. It serves well for the MNSR core. To properly define the source, a distribution of energies is needed, as well as the radius and length of the cylinder and its position. The option “erg” defines the energy, “rad” the radius, “ext” the length, “par” the source particle type, “pos” the location, and “axs” the orientation of the cylinder axis. “d1”, “d2” and “d3” are distributions of values that the code uses as input for the different options.

Due to the fact that the dose rate had to be determined at different positions as it is unloaded from the core, the TR (Coordinate transformation) card was used to move the SNF cage to the different location from the bottom of the reactor vessel.

SPn (Source probability) card, which was also used, defines a source probability. The parameter “-2” corresponds to an already built in function of a Maxwell fission spectrum. Hence, “SP1 -2” assigns the Maxwell spectrum to the distribution of initial energies of the source.

SIn (Source Identification) card defines the true distribution of the SPn card. It set the bin boundaries. The values are either of the source variables or distribution number in this case, the energies of the photon spectrum was used in the sp2 card. “SI2 r1 r2” defines a uniform distribution between radius r1 and r2. SI3 works in the same way defining the boundaries of cylinder height.

The “pos” which is the reference point for position sampling is usually stated in the x y z coordinates of the center of the cylinder is the position where the particles start. The “axs” gives the direction of the x y z vector of the cylinder axis. In this case, the cylinder was pointing upwards. Finally, “par” is used to describe the particle that the source will emit. For this work, par = 2 indicating that photon was emitted.

The d1 distribution represents the radial flux distribution profile of the fuel pin arranged in ten (10) concentric circles (rings). The normalized ring flux relative to the average pin flux was used as input in the deck

The d3 distribution which is the axial segment flux profile of the ten concentric circles works basically in the same way d1 did. Normalization of the axial values works the same way as that in d1.

The d2 distribution represents the energy distribution. This input was picked from the ORIGEN-S output for gamma radiation in photons/second for the 39-energy groups (see Appendix A.2). The source strength for the total cooling time for the 39-energy group was also used as the source term for calculating the dose rate [33] [40].

The flowchart as illustrated in fig 4.1 explains the processes taken and the points at which the various codes were used in this work.

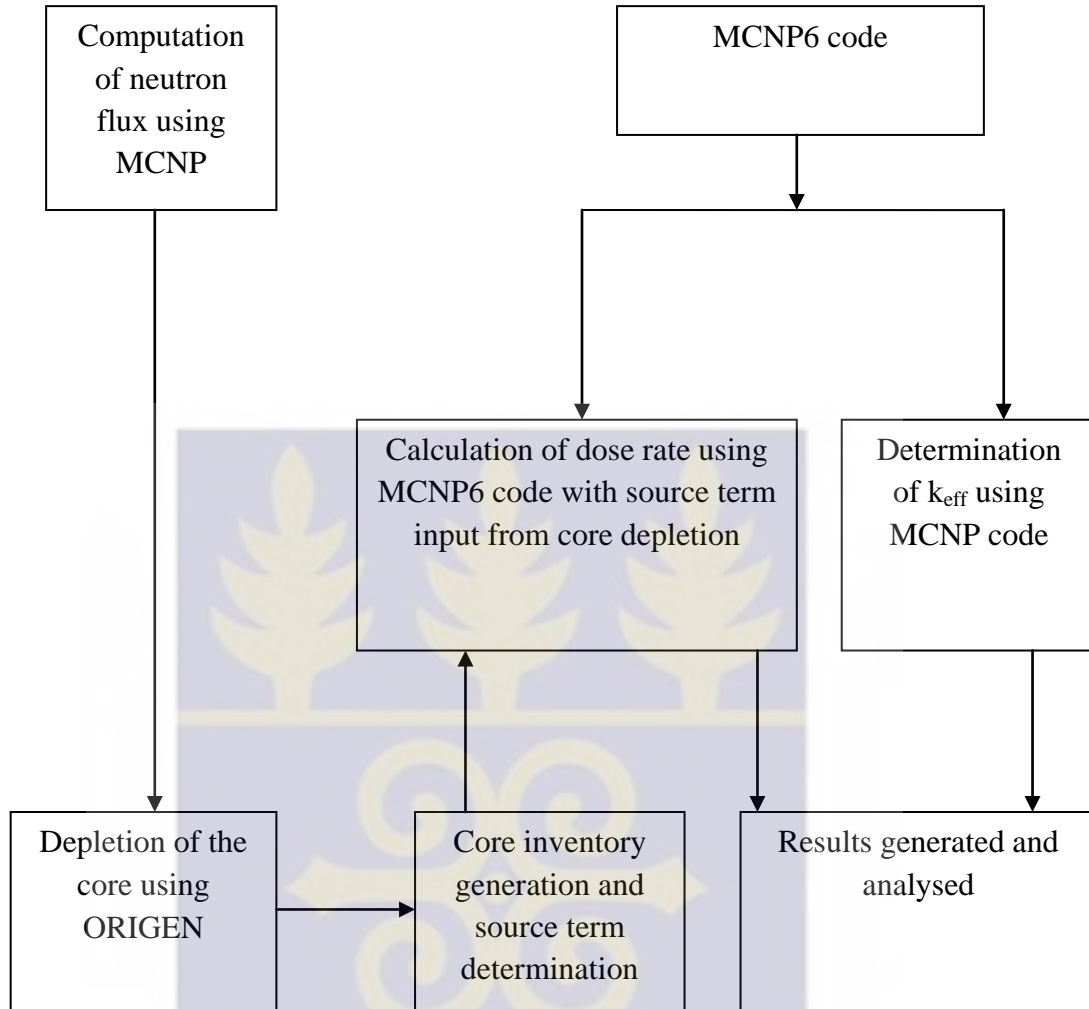


Fig 4.1: Flow chart illustrating methodology

During the lifting of the cage, the radiation dose and criticality was determined at various heights from the bottom of the reactor vessel. MCNP6 was used to mimic the core at various levels and are presented pictorially as shown in fig 4.2 to fig 4.7.

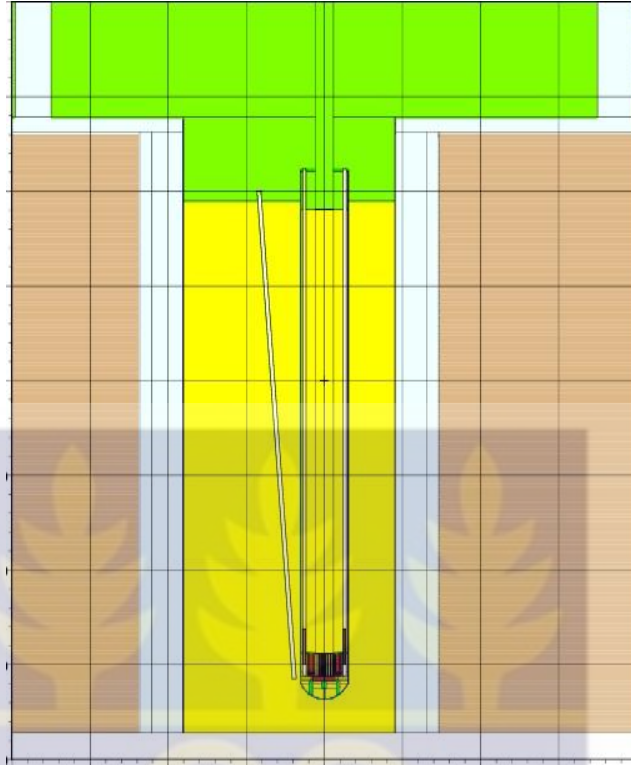


Fig.4.2: Fuel Cage Center at the bottom of core 0.0 cm

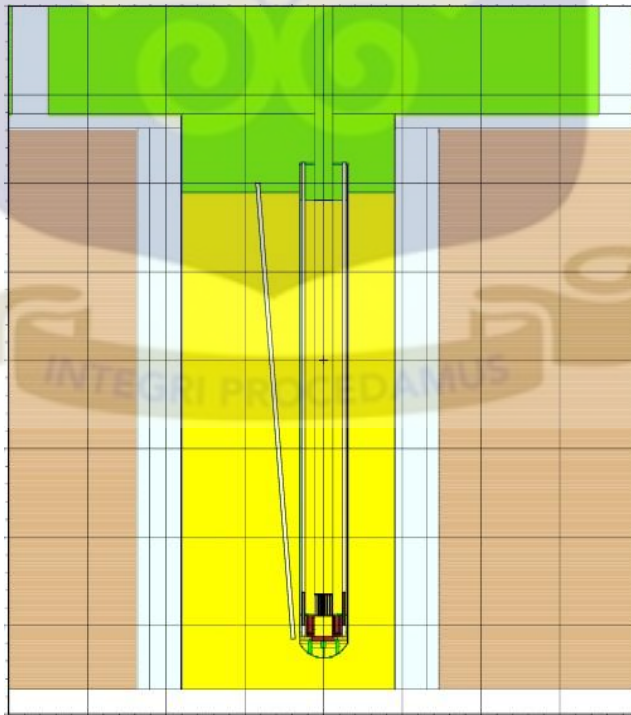


Fig. 4.3: Fuel Cage Center at 24.6 cm above bottom

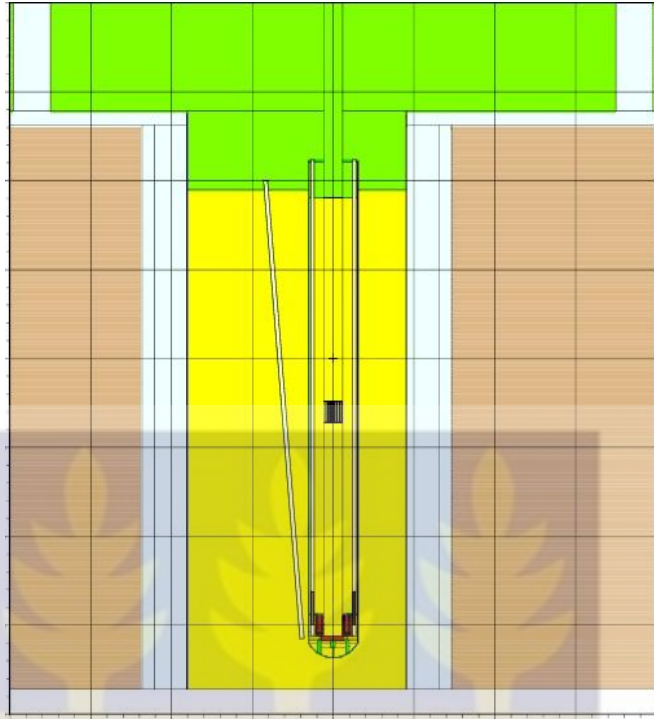


Fig.4.4: Fuel Cage Center at 240 cm above bottom

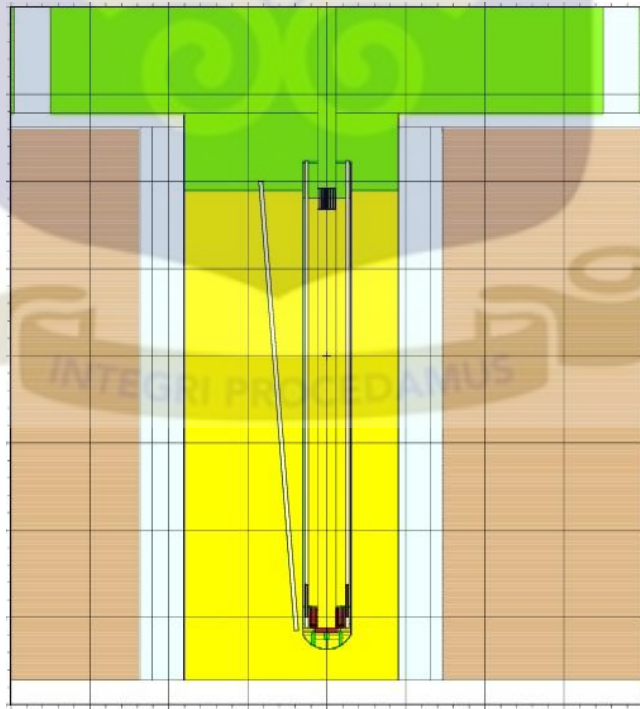


Fig.4.5: Fuel Cage Center at 480 cm above bottom

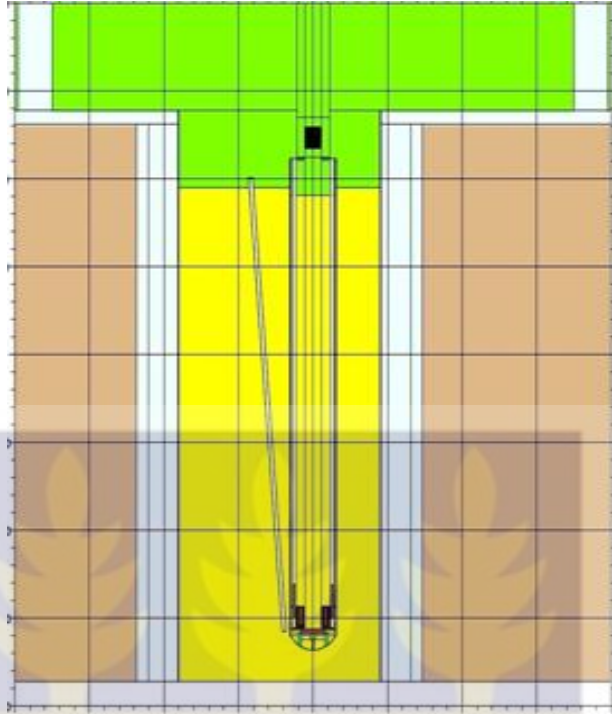


Fig.4.6: Fuel Cage Center at 495 cm above bottom

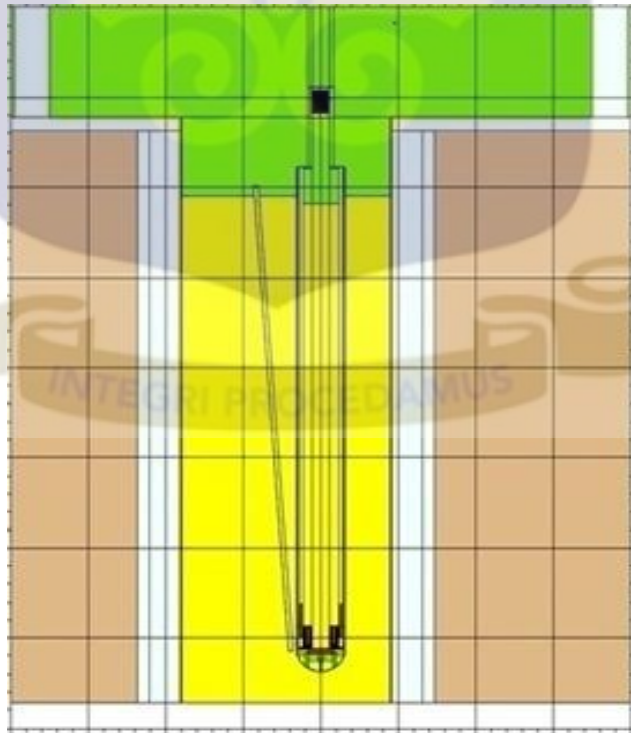


Fig. 4.7: Fuel Cage Center at 595 cm above bottom

The computational tools used were useful in the determination of the core inventory, estimation of the dose rate and the calculation of the criticality of the core of GHARR-1.

The results obtained from the runs are discussed in the next chapter.



CHAPTER FIVE

5 RESULTS AND DISCUSSION

In dose calculation as well as criticality safety analysis, the isotopic components of the Spent Nuclear Fuel are of great importance. This chapter looks at the results from the codes used for depleting the core of GHARR-1 and also the estimation of the radiation dose rate. Further analysis and discussions are also made.

5.0 CORE INVENTORY OF NUCLEAR FUEL OF GHARR-1

The isotopic component of the core which was obtained by the depletion of the HEU core was useful in determination of the source term.

The inventory of a reactor fuel depends on a number of factors. These factors include the quantity of the fissile material, the reactor type and the reactor design. Other factors comprise fuel power and burnup, neutron flux in the core, operational history, fuel management, decay time after shut down as well as production of particular isotopes. The large number of radionuclides that are formed during the fission process can be grouped into small sets of categories based on their physical and chemical characteristics. The radioactive nuclides were therefore classified into light element from the cladding, fission products from some specific fissile materials and actinides from the fuel. Tables 5.1 to 5.3 give an outline of the various radionuclide and their corresponding concentrations.

Table 5.1: Inventory of some important radionuclides in the Actinide group

Radionuclide	Activity (Curies)
U-237	3.13E-01
U-235	2.12E-03
U-235m	1.72E-06
Pu-238	3.74E-05
Pu-239	5.04E-03
Pu-240	8.47E-05
Pu-241	3.17E-04
Np-238	1.06E-03
Np-239	1.48E+01
Np-240m	9.31E-12
Am-241	2.75E-06
Am-242m	3.18E-09
Am-242	1.75E-06
Th-230	1.32E-05
Th-229	8.31E-11
Th-231	2.43E-03
Cm-242	1.08E-06

Table 5.2: Inventory of some important radionuclides in the Light Element group

Radionuclide	Activity (Curies)
Fe-55	2.87E-02
Fe-59	8.95E-04
Fe-60	1.60E-14
Co-58	2.89E-03
Co-60	2.02E-05
Co-60m	1.18E-11
Al-26	1.36E-08
Al-28	1.46E-05
Al-29	9.44E-11
B-12	2.06E-12
C-14	1.25E-05
Zn-65	2.04E-04
Zn-69	1.19E-05
He-6	3.58E-12
N-24	1.92E-01
N-22	1.38E-11
H-3	2.04E-01
Be-8	1.54E-11
Be-10	8.51E-11
Be-11	1.18E-15
K-40	2.92E-12
K-42	6.84E-08
Li-8	1.43E-10
Ar-41	8.40E-12
Ar-42	8.51E-14
Mg-28	4.40E-11
S-35	1.24E-13
Si-32	1.32E-14
Ca-41	5.09E-08

Table 5.3: Inventory of some important radionuclides in the Fission Products group

Radionuclide	Activity (Curies)
Br-82	1.65E-03
Br-82m	5.03E-10
Br-84	8.33E-06
Br-84m	1.45E-07
I-131	3.92E+01
I-132	6.86E+01
I-132m	4.67E-05
I-133	1.03E+02
I-134	6.32E-04
I-135	3.69E+01
I-136	2.34E-05
Xe-133	9.63E+01
Xe-135	1.06E+02
Xe-137	5.24E-05
Xe-138	5.43E-05
Kr-85m	3.56E+00
Kr-87	5.58E-03
Kr-88	2.15E+00
Kr-89	3.89E-05
Sr-89	5.46E+01
Pm-147	2.33E+01
Cs-136	8.27E-02
Cs-137	2.46E+01
H-3	7.42E-02
Ba-137m	2.33E+01
Ba-136m	9.15E-03
Ba-140	8.02E+01

The nuclides of interest in source term calculations are volatile and semi volatile nuclides since these are likely to be released from a heated fuel element. The most volatile ones include Xe, I, Kr, Cs and Te. The actinides and fission products have much higher boiling points; hence, they remain dissolved in the fuel. Precursor sources for nuclides of interest such as iodine can be determined from their decay chain and yields. For research reactors, the amount of activity of the other radionuclides other than fission products is significantly less than that of activation products and thus their contribution is not significant. With special irradiation devices, possible significant amounts of radionuclides may be formed. Some of the radionuclides may be in gaseous or liquid form for which the probability of a release may be more significant than with solid activation products, (e.g. Ar-41)

The light elements possess small atomic numbers and have a short half-life in second to a few days.

Actinides mostly have long lived radionuclides. They usually split to form fission products with the release of neutron to continue the chain reaction. U-238 undergoes a neutron capture to form U-239, which quickly decays by β -emission to become Np-239. Further transmutations of the Np-239 lead to even higher actinides and other fission products. The major contributor to the actinide are Np-239 and U-237 which are short-lived radionuclides with half-lives in the order of days but will decayed to form Pu-238 and Pu-239 which has longer half-lives.

Fission products are the atomic fragments left after a large atomic nucleus undergoes nuclear fission. For instance, Uranium fissions by splitting into two smaller nuclei, along

with a few neutrons, the release of heat energy and gamma rays. The fission products with short half-life (a few like I-129 and Cs-135 are long lived), are often unstable and radioactive because they possess more neutrons than a stable atom with the same atomic number. The initial fission products which are unstable undergo beta decay to become stable by converting a neutron to a proton with each beta emission. The first beta decay happens quickly with the release of high energy gamma radiation. As the fission products become stable, the last decay processes may have a long half-life and release less energy.

5.0.1 Source term estimation

The gamma source intensity during cooling from day 0 to 180 days after discharge is tabulated in Table 5.4 at a power of 15kW

Table 5.4: Gamma source intensity during the cooling cycle after shut down

No. of days	Gamma Source Intensity *10 ¹³ (photons/sec)
0	10.11
0.04	9.859
0.2	9.19
0.5	7.904
1	6.729
5	3.975
10	2.972
30	1.767
60	1.237
90	0.9906
180	0.63565

The amount of photons in the nuclides decreased with an increase in the number of days because there is a slower or no rate of photon production as the nuclides becomes stable. Thus the total radioactivity of the of the core decreases rapidly for the first few days (this is controlled by the short lived nuclides such as I-131, Ba-140 and SR-90) before stabilizing to a low level with the change in radioactivity becoming gradual (controlled by the long lived nuclides such as Sr-90,Cs-137) and lasts for many more years.

The cooling of the core was done to aid the removal of the heat generated as a result of the continuous nuclear reaction prior to shutdown, was monitored for 180 days after shut down. After 180 days, most of the nuclides would have decayed and their relevance to the dose rate would have been lost because every little nuclide is of importance to the overall dose rate. With reference to Appendix A.1, the source strength at 30 days after shutdown was used to calculate the dose rate. This is because after 30 days, most of the radionuclides would have decayed or transmuted into other stable nuclides with shorter half lives. The source term of 1.767×10^{13} photons/sec was taken at 30 days at 15kW with an effective energy calculated by the ORIGEN-S code to encompass all the very important radionuclides such as Xe which is related to the burnup of the core. These radionuclides will still be prominent in the inventory after this time.

5.1 RADIATION DOSE RATE AND CRITICALITY FROM MCNP

The total radiation that the personnel would be exposed to during the core removal will be the absorbed dose in tissue given off at the point of discharge. The unit for the absorbed dose is Gray (Gy). Since dose to human is measured in mSv (millisievert), there

is the need to establish the relationship between the Gy and Sv. One gray of gamma radiation is equivalent to one Sv of biological effects.

Radiation damage depends on the absorption of energy from the radiation and is approximately proportional to the mean concentration of absorbed energy in irradiated tissue. For this reason, the basic unit of radiation dose is expressed in terms of absorbed energy per unit mass of tissue. The result of the photon dose was in mrem/hr and was converted to mGy (absorbed dose) using the conversion factor

$$100\text{mrem} / \text{hr} = 1\text{mGy} / \text{hr} \quad (5.1)$$

$$1\text{mrem} / \text{hr} = 1 \times 10^{-2} \text{mGy} / \text{hr} \quad (5.2)$$

For the purpose of assessing the bounding radiological consequences of a release of actinides from fuel material, the maximum doses would be obtained at the time of discharge.

5.1.0 Results from MCNP6 dose rate estimation

Dose rate at the various points from the bottom of the vessel to the top were estimated. Tables 5.5 to 5.13 shows the results as obtained from the output and their conversion to mGy/hr from mrem/hr.

Table 5.5: Dose rate at various heights above the bottom of core with detector above the reactor floor

Detector Above the reactor core-floor level		
Height above the bottom (pz)(cm)	mrem/hr	mGy/hr
0	6.61E-08	6.61E-10
24.6	8.61E-04	8.61E-06
240	2.54E-02	2.54E-04
480	1.05E+05	1.05E+03
595	4.27E+06	4.27E+04

Table 5.6: Dose rate at various heights above the bottom of core with detector towards the control room

Detector on the Fence towards control room		
Height above the bottom (pz)(cm)	mrem/hr	mGy/hr
0	2.73E-14	2.73E-16
24.6	2.03E-05	2.03E-07
240	1.53E-05	1.53E-07
480	2.61E+02	2.61E+00
595	1.19E+04	1.19E+02

Table 5.7: Dose rate at various heights above the bottom of core with detector away from the control room

Detector on the Fence away from control room		
Height above the bottom (pz)(cm)	mrem/hr	mGy/hr
0	8.69E-15	8.69E-17
24.6	3.03E-05	3.03E-07
240	1.90E-05	1.90E-07
480	2.02E+02	2.02E+00
595	2.55E+04	2.55E+02

Table 5.8: Dose rate at various heights above the bottom of core with detector towards the door

Detector on the Fence towards door		
Height above the bottom (pz)(cm)	mrem/hr	mGy/hr
0	1.40E-14	1.40E-16
24.6	2.07E-05	2.07E-07
240	1.59E-05	1.59E-07
480	2.35E+02	2.35E+00
595	1.59E+04	1.59E+02

Table 5.9: Dose rate at various heights above the bottom of core with detector at the door

Detector At door		
Height above the bottom (pz)(cm)	mrem/hr	mGy/hr
0	6.92E-16	6.92E-18
24.6	1.63E-05	1.63E-07
240	1.24E-05	1.24E-07
480	1.61E+02	1.61E+00
595	8.55E+03	8.55E+01

Table 5.10: Dose rate at various heights above the bottom of core with detector at the Control room window

Detector at Control room window		
Height above the bottom (pz)(cm)	mrem/hr	mGy/hr
0	2.86E-15	2.86E-17
24.6	1.70E-05	1.70E-07
240	3.77E-06	3.77E-08
480	1.49E+02	1.49E+00
595	8.21E+03	8.21E+01

Table 5.11: Dose rate at various heights above the bottom of core with detector at the Rabbit room window

Detector at the Rabbit room window		
Height above the bottom (pz)(cm)	mrem/hr	mGy/hr
0	3.51E-23	3.51E-25
24.6	8.98E-15	8.98E-17
240	1.24E-13	1.24E-15
480	1.18E-01	1.18E-03
595	3.83E+00	3.83E-02

Table 5.12: Dose rate at various heights above the bottom of core with detector at the Far side of room

Detector at the Far side of room		
Height above the bottom (pz)(cm)	mrem/hr	mGy/hr
0	1.27E-16	1.27E-18
24.6	2.26E-05	2.26E-07
240	9.75E-06	9.75E-08
480	1.37E+02	1.37E+00
595	7.35E+03	7.35E+01

Table 5.13: Dose rate at 595cm above the bottom of core with detector placed at different positions

Detector placed 595 cm above the bottom of core		
Position	mrem/hr	mGy/hr
Above the reactor core- floor level	4.27E+06	4.27E+04
Fence towards control room	1.19E+04	1.19E+02
Fence away from control room	2.55E+04	2.55E+02
Fence towards door	1.59E+04	1.59E+02
At the door	8.55E+03	8.55E+01
Control room window	8.21E+03	8.21E+01
Rabbit room window	3.83E+00	3.83E-02
Far side of room	7.35E+03	7.35E+01

Radiation dose rate varies as a function of SNF's assembly burnup, initial enrichment, and decay time. The amount of radiation an individual receives will also depend on how close the person is to the source, the time spent close to the source as well as the shielding available. Thus the distance at which the detector is placed away from the source is also a factor that contributes to the radiation dose.

As the cage is moved from the bottom to the top, the cage gets closer to the detector and thus more photons are incident on the detector. With the increase in photons, the dose rate also increases.

The radiation dose as the cage is in the reactor vessel is low because at the bottom, the annular Beryllium reflector and lower beryllium slab, reflects the photons back into the cage whereas the coolant also acts as a shield, thereby attenuating the radiation intensity. The distance between the cage and the detector too is far and thus the low values for the dose rate at the bottom.

At the height just above the beryllium reflector the coolant again serves as a shield and the distances between the detector and the cage will have reduced, thus increasing the photons intensity and in effect increasing the dose rate.

This increase in photons emitted is progressive as the cage is moved to the top whereas the distance between the detector and cage reduces, thus the dose rate increases as well. With the cage just at the top, where part of the cage is in the vessel and the other half in air, the shielding is reduced and most of the photons are incident on the detector with the distance also closing up.

When the cage finally out of the vessel, the radiation source becomes unshielded and as such the photons are scattered in all directions. The photon intensity is highest at this point because the distance between the cage and detector would be short thus increasing the radiation dose rate.

From Table 5.13, it can also be concluded that the distance between the cage (radiation source) and the detector contributes to the dose rate. At the rabbit room which is the farthest position from the reactor vessel, the dose rate is **3.83E-02mGy/hr** which is the smallest as compared to the dose rate of **4.27E+04mGy/hr** when the detector was above the reactor vessel.

The maximum values of the dose rate at the various positions where the reactor was placed proves that they fall within the acceptable limit set by NRC and stated in SAR (GHARR-1). The allowable radiation dose of 20 millisievert per year averaged over five years with a maximum of 50 millisievert in any one year will be attained if the methods of protection are adhered to.

5.1.1 Criticality (k_{eff}) calculations

Neutrons are not emitted as a direct result of natural radioactive decay but they are formed as a result of nuclear reactions. In nuclear fuel, the Uranium nuclide disintegrates to form other fission fragments and approximately two and a half new neutrons.

As the fuel becomes spent, it's unable to sustain this chain reaction and thus there will be a decrease in the neutron population. The neutron population decreased as the cage was moved towards the top of the vessel. The factor that was varied was the distance above the bottom of the vessel. At the bottom, the presence of the moderator slows down the fast neutrons whilst the lower beryllium slab and the annular beryllium reflector reflect the neutrons back into the cage thus increasing the population of the neutrons.

The presence of the cadmium rabbits (capsules) which was pumped into the irradiation channels before core removal will serve as neutron absorbers thus the reducing the criticality at the bottom of the vessel to less than unity

As the cage was moved to the top, the population of neutrons reduced because the conditions suitable for criticality to be high such as reflectors were absent thereby reducing criticality. Another important factor is the fact that the core of GHARR-1 is small and as such neutron leakage is high. Also there is no reflector to reflect escaping

neutrons from the small core. This explains why with the cage totally in air, the criticality is **0.01238**.

The values obtained are presented in the table 5.14

Table 5.14: Criticality values as the cage is being lifted to the top of the vessel

Cage height (cm)	k_{eff}
0.00	0.99442
24.6	0.84829
240	0.84381
480	0.60202
495	0.05085
595	0.01238

For a system to remain sub-critical, k_{eff} should be less than 1. The results prove that the Nuclear Fuel will remain sub-critical as long as it stays out of the reactor. The results as compared to Odoi, 2014, [25] and Moustafa et al, 2000, [42], were in good agreement with the safety of the NF which is to be kept at a sub-critical state during off-site conditions.

The results obtained have been analysed and they were in better agreement with international standard and earlier works. The next chapter will draw conclusion on the results from this study.

CHAPTER SIX

6 CONCLUSION AND RECOMMENDATION

6.0 CONCLUSION

International concerns on the use of HEU powered reactors for peaceful use has necessitated the conversion program for GHARR-1's fuel under the IAEA-RERT. With the conversion of the core of GHARR-1 reaching its implementation stage, there is therefore the need to carry out this study to anticipate the radiation dose that the personnel will be exposed to during the program.

With a reactor power history of 15kW, the reactor was operated for eleven months in a year, four weeks in a month, four days in a week and four hour every day. The operational history of the reactor was observed for the last 20 years through to the last five days of the cycle before the core was shutdown to establish the nuclide composition of the core.

At the end of the irradiation period, the results showed that the core comprised nuclides grouped into light elements, actinides and fission products. The concentration of the nuclides ranged between 2.930×10^{-28} curies and 1.059×10^{-2} curies at discharge. U-237 and Pu-240 which are the most important nuclides of the NF of the MNSR had relatively low concentration as compared to the concentration needed for nuclear weapons proliferation. Thus GHARR-1 can be viewed as a safe reactor in terms of proliferation.

A source term of 1.767×10^{13} photons/sec at 30 day after cooling was used to estimate the dose rates of the core. The dose rates increased from 3.51×10^{-25} mGy/hr to 4.27×10^{-4} mGy/hr at various heights during the lifting. The progressive increase was due to

the reduction in the shielding and the closeness of the detector to the source (cage) in terms of distance. Thus the dose rates clearly explain the principles of shielding in terms of distance and shield.

The dose rates were in good agreement with dose limits as stated in the Ghana Research Reactor-1 Safety Analysis Report (SAR) by Akaho et al [26], the safe dose limits to the personnel should be 20mSv/year averaged over five consecutive years or 50mSv/year in every single year. For pre-planned special exposure, the dose received by an individual should not exceed 100mSv per the event and also not more than 250mSv in one's life time [26]. The dose rates when the cage was hanging in air were too high, which were beyond the dose limits thus it will be prudent for the core unloading to be done remotely with personnel monitoring the process from the control room until the cage is put in a transfer cask which will further reduce the dose rate exposure. The highest dose rate in the control room which was monitored with the detector placed on the window was 8.21×10^1 mGy/hr, which is within the dose rate limit specified for pre-planned special exposure.

For the general public, the dose limit is 1mSv per year which excludes the dose contributed from background radiation.

The criticality of the Nuclear Fuel (HEU fuel) was also determined during the core unloading to ascertain whether the nuclear fuel (NF) will remain sub-critical after it is unloaded. According to the Safety Standards of the International Atomic Energy Agency (IAEA) decommissioned nuclear fuel should be kept at a sub-critical level to ensure that nuclear fission chain is not sustained. The k_{eff} values decreased from 0.99442 to 0.01238

which indicated that the core will remain sub-critical thus will never become critical in the course of removal.

The results from this research work were consistent with the findings of earlier works[3][25][38] and the accepted dose limits of 50mSv per year and 100mSv for pre-planned exposure as adopted by the Ghana Nuclear Regulatory Authority (NRA) and stated in GHARR-1 Safety Analysis Report (SAR).

6.1 RECOMMENDATION

After the completion of this research work, I recommend the following

- Even though the doses are minimal except for the dose rate when the core is hanging in air, shielding (transfer cask) should be provided when the cage is hanging in air.
- Shielding gears such as Lead aprons should be worn as well as the use of electronic personal detectors like the pocket dosimeter, film badges to further protect personnel against the radiation dose
- Background radiation should be monitored at all times
- Monitors should be used to observe the activities in and around the control room to observe activities during the core unloading
- Detectors such as He-detector (for fast neutrons) and Ionizing chambers (for thermal and epithermal neutrons) should be used to monitor any abnormal dose excursions as a result of core removal.

- A radiation safety plan that outlines all radiation activities involved in the removal should be put in place.
- Access to the reactor room should be restricted to only the personnel involved in the core unloading. That is the reactor room should be cordoned to prevent unauthorized person from entering the area



REFERENCES

- [1] International Atomic Energy Agency (IAEA), www.iaea.org/About/policy/GC/GC48/documents/gc48inf.4_ftnl.pdf
- [2] Abrefah R.G., Neutronics and Dose Calculation for Prospective Spent Nuclear Fuel Cask for Ghana Research Reactor-1 Facility, A Dissertation presented to The Department of Nuclear Engineering, School of Nuclear and Allied Sciences, and published by The University of Ghana in Partial fulfillment for Doctor of Philosophy (Phd) in Nuclear Engineering, 2014
- [3] Briemeister J.F., "MCNPTM-A General Monte Carlo N-Particle Transport Code," Version 4c Manual, Vols. LA-13709-M, USA: LANL, 2000.
- [4] McKinney G., "A Practical Guide to Using MCNP with PVM," Trans. Am. Nuclear Soc., no. 71, p. 397, 1994
- [5] International Atomic Energy Agency, International Atomic Energy Agency Bulletin, vol. 3, p. 35, 1993
- [6] Committee on the current Status of and progress Towards Eliminating Highly Enriched Uranium use in Civilian Research and Test Reactors: Nuclear and Radiation Studies Board, Division of Earth and Life Science, National Academies of Science, Engineering and Medicine, Reducing the Use of Highly Enriched Uranium in Civilian Research Reactors
- [7] Jordi R.R. and Christopher L., Research and Test Reactor Conversion to Low Enriched Uranium Fuel: Technical and Programmatic Progress. International Conference on Research Reactors: Safe Management and Effective Utilization, Rabat, 2011

- [8] IAEA Safety Standards Series No.GSG-1, Classification of Radioactive Waste General Safety Guide Vienna, 2009
- [9] IAEA, "Safety and Engineering Aspects of Spent Fuel Storage," Proceedings of an International Symposium on Safety and Engineering Aspects of Spent Fuel Storage jointly organised by IAEA and NEA (OECD), Vienna, 1994,
- [10] Lamarsh J.R., Baratta A.J., Introduction to Nuclear Engineering, Third Edition, Prentice-Hall, 07458, 2001
- [11] Odoi, H.C., Gbadago, J.K., Abrefah, R.G., Birikorang, S.A., Sogbadji, R.B. M, Ampomah-Amoako E., Efforts made for the Conversion of Ghana's MNSR to LEU. International meeting on Reduced Enrichment for Research and Test Reactors IAEA, VIC, Vienna, Austria, 2014.
- [12] Marques J.G., Technical University of Lisbon, Core Conversion of the Portuguese Research Reactor, Instituto Tecnológico e Nuclear, Estrada Nacional 10, P-2686-953 Sacavém, Portugal, RERTR 2007 International Meeting, 2007
- [13] Dennis H., Puig F., Neutronic Analysis of the Jamaican SLOWPOKE-2 Research Reactor for the Conversion from HEU to LEU fuel Technical Meeting on Enhanced Utilization of Zero Power Reactors and Subcritical Assemblies Bariloche, Argentina, 2014.
- [14] Grant C. and Preston J., Progress Report on Activities for the Core Conversion in Jamaica, International meeting on Reduced Enrichment for Research and Test Reactors Warsaw, Poland, 2012.

- [15] Grant C., International Centre for Environmental and Nuclear Sciences University of the West Indies Regional Practical Workshop on the Decommissioning of Radioactively Contaminated Facilities: NECSA South Africa, 2011
- [16] Dennis H., Puig F., Analysis of the Jamaican Slowpoke-2 Research Reactor for the conversion from HEU to LEU fuel, RERTR 2014 — 35th International Meeting on Reduced Enrichment for Research and Test Reactors, IAEA Vienna International Center Vienna, Austria, 2014
- [17] Toth G, Benkovics I., HEU-LEU Core Conversion at Budapest Research Reactor, Center for Energy Research, Hungary, 2014
- [18] Pond R. B., Hanan N. A. and Matos J. E. and Maraczy C., A Neutronic Feasibility Study for LEU Conversion Of The Budapest Research Reactor, Presented at the 1998 International Meeting on Reduced Enrichment for Research and Test Reactors Sao Paulo, Brazil, 1998
- [19] <http://www.euronuclear.org/e-news/e-news-50/issue-50-print.htm>, Feb 2016
- [20] Toth G., Decommissioning Activities of Budapest Research Reactor RER3009/9019/01 Safety Assessment for Decommissioning of Research Reactors (R²D²P), Roskilde, Denmark, 2010
- [21] Tozsér S. Full-scale reconstruction and upgrade of the Budapest Research Reactor, Hungarian Academy of Sciences, KFKI Atomic Energy Research Institute, Budapest, Hungary
- [22] Radulescu G., Lefebvre R.A., Peplow D.E., Williams M.L. Scaglione J.M., Dose Rate Analysis Capability for Actual Spent Fuel Transport Cask Content Institute

- of Nuclear Materials Management (INMM)–55th Annual Meeting Atlanta, Georgia USA, 2014
- [23] Pond R.B. and Matos J.E., Photon dose rate from Spent Fuel Assemblies with Relation to Self-Protection, Argonne National Laboratory, 1996
- [24] Pond R.B. and Matos J.E., Nuclear Mass Inventory, Photon Dose Rate and Thermal Decay Heat Of Spent Research Reactor Fuel Assemblies, Argonne National Laboratory, Seoul, Korea, 1996
- [25] Odoi H.C., Reactor Core Conversion Studies of Ghana Research Reactor -1 and Proposal for Addition of Safety Rod, A Dissertation presented to The Department of Nuclear Engineering, School of Nuclear and Allied Sciences, and published by The University of Ghana in Partial fulfillment for Doctor of Philosophy (Phd) in Nuclear Engineering, 2014
- [26] Akaho, E.H.K., Anim-Sampong, S., Dodoo-Amoo, D.N.A., Maaku, B.T., Emi-Reynolds, G., Osa, E.K., Boadu, H.O., Bamford, S.A., 1995. Safety Analysis Report for Ghana Research Reactor-1, GAEC-NNRI-RT-26, March 1995.
- [28] Parks C.V., Overview of ORIGEN2 and ORIGEN-S: Capability and Limitations, 1992 International High-Level Radioactive Waste Management Conference, 1992
- [29] Oak Ridge National Laboratory, Scale: A Comprehensive Modeling and Simulation Suite for Nuclear Safety Analysis and Design ORNL/TM-2005/39 Version 6.1, 2011

- [30] Ball S. J. and Adams R. K., MATEXP: A General Purpose Digital Computer Program for Solving Ordinary Differential Equations by the Matrix Exponential Method, ORNL/TM-1933, Union Carbide Corporation (Nuclear Division), Oak Ridge National Laboratory, Oak Ridge, Tenn, 1967.
- [31] Lapidus L. and Luus R., Optimal Control of Engineering Processes, Blaisdell Publishing Co., Waltham, Mass., 1967, pp. 45–49.
- [32] Lee C. E., The Calculation of Isotopic Mass and Energy Production by a Matrix Operator Method, LA-6483-MS, Los Alamos Scientific Laboratory, 1976
- [33] X-5 Monte Carlo Team, "MCNP—A General Monte Carlo N-Particle Transport Code," Los Alamos National Laboratory, USA, Los Alamos, Version 5 Edition, 2005
- [34] Los Alamos National Laboratory, RSICC Computer Code Collection, MCNP6.1/MCNP5/MCNPX
- [35] Brewer R., X-1 TA, Criticality calculations with MCNP5: A Primer, LA-UR-09-00380, Los Alamos National Laboratory, 2009
- [36] Carter L.L. and Cashwell E.D., "Particle Transport Simulation with the Monte Carlo Method," in ERDA Critical Review Series, TID-26607, 1975
- [37] Spriggs G.D., Busch R.D., Adams K.J., Parsons D.K., Petrie L., and Hendricks J.S., "On the Definition of Neutron Lifetimes in Multiplying and Non multiplying Systems," Los Alamos National Laboratory Report, LA-13260-MS, 1997.

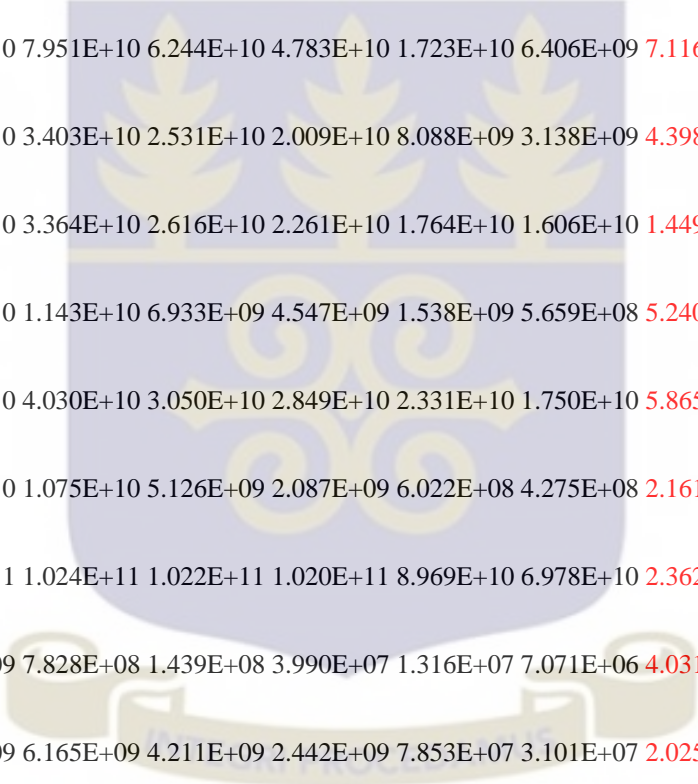
- [38] Hermann O.W., Westfall R.M., ORIGEN-S: Scale System to Calculate Fuel Depletion Actinides Transmutation, Fission Products Buildup and Decay and Associated Radiation Source Terms, NUREG/CR-0200, Section 7, ORNL/NUREG/CSD-2/V2/R/ 1998
- [39] Abrefah R.G., Birikorang S.A., Nyarko B.J.B., Fletcher J.J., Akaho E.H.K. National, Design of serpentine cask for Ghana research reactor-1 spent nuclear fuel, Progress in Nuclear Energy Volume 77, 2014, Pages 84–91 2014
- [40] Shultis J.K. and Faw R.E., "An MCNP Primer", Manhattan-Kansas: Department of Mechanical and Nuclear Engineering, Kansas State University, Manhattan, KS66506, 2011
- [41] Glastone S. and Sesonske A., "Nuclear Reactor Engineering, Reactor Design Basics", Fourth Edition, Vol. 1, Publisher, Springer 1994, ISBN 10: 0412985314, 1994
- [42] Aziz M. and Andrzejewsk K., Criticality calculations for the spent fuel storage pools for Etrr_1 and Etrr_2 reactors, Nukleonika 2000; 45(2):141–144, 2000
- [43] Brown F.B., X05, Fundamentals of Monte Carlo Particle Transport, Los Alamos Laboratory
- [44] www.nrc.gov/about-nrc/regulatory/research/safetycodes.html
- [45] International Atomic Energy Agency, "Nuclear Power, Nuclear Fuel Cycle and Waste Management: Status and Trends," in IAEA Yearbook, Vienna, IAEA, 1994, p. Part C

APPENDIX

Appendix A.1 Gamma Source intensity during the decay period

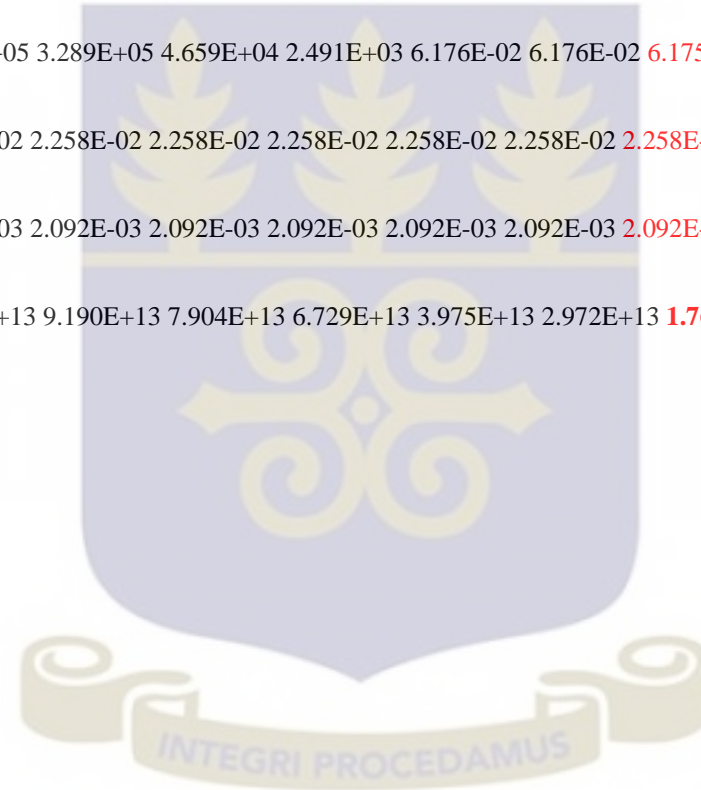
gamma source intensity as a function of time 0		GHARR-1 HEU344 CORE DECAY AFTER SHUTDOWN TO 180										
DAYS IN 10 STEPS		gamma spectra, photons/sec/basis							basis = 0.001101 MTU			
grp	boundaries, mev	0.0 d	4E-02 d	0.2 d	0.5 d	1.0 d	5.0 d	10.0 d	30.0 d	60.0 d	90.0 d	180.0 d
1	0.00E+00 - 1.00E-03	1.394E+07	1.384E+07	1.358E+07	1.310E+07	1.271E+07	1.212E+07	1.188E+07	1.119E+07	1.047E+07	9.967E+06	8.967E+06
2	1.00E-03 - 5.00E-03	3.791E+12	3.701E+12	3.467E+12	3.039E+12	2.660E+12	1.696E+12	1.281E+12	7.363E+11	5.091E+11	4.176E+11	3.004E+11
3	5.00E-03 - 1.00E-02	9.508E+12	9.199E+12	8.410E+12	7.024E+12	5.904E+12	3.843E+12	3.209E+12	2.253E+12	1.723E+12	1.462E+12	1.072E+12
4	1.00E-02 - 5.00E-02	2.124E+13	2.073E+13	1.943E+13	1.696E+13	1.468E+13	8.551E+12	6.214E+12	3.632E+12	2.634E+12	2.196E+12	1.595E+12
5	5.00E-02 - 1.00E-01	6.284E+12	6.134E+12	5.751E+12	5.064E+12	4.468E+12	2.825E+12	2.016E+12	1.055E+12	7.728E+11	6.613E+11	4.958E+11
6	1.00E-01 - 2.00E-01	8.082E+12	7.925E+12	7.521E+12	6.761E+12	6.014E+12	3.489E+12	2.454E+12	1.520E+12	1.042E+12	7.970E+11	5.023E+11
7	2.00E-01 - 3.00E-01	9.069E+12	8.774E+12	7.951E+12	6.193E+12	4.484E+12	1.315E+12	6.042E+11	2.336E+11	1.770E+11	1.528E+11	1.148E+11
8	3.00E-01 - 4.00E-01	3.112E+12	3.064E+12	2.940E+12	2.709E+12	2.486E+12	1.692E+12	1.196E+12	3.998E+11	1.627E+11	1.177E+11	8.620E+10

9	4.00E-01 - 5.00E-01	2.969E+12	2.936E+12	2.856E+12	2.726E+12	2.623E+12	2.198E+12	1.783E+12	8.444E+11	3.666E+11	2.057E+11	7.164E+10
10	5.00E-01 - 6.00E-01	7.166E+12	6.917E+12	6.251E+12	4.927E+12	3.700E+12	1.491E+12	1.097E+12	5.565E+11	2.848E+11	1.764E+11	7.035E+10
11	6.00E-01 - 7.00E-01	8.184E+12	8.067E+12	7.598E+12	6.414E+12	5.161E+12	2.177E+12	1.368E+12	9.241E+11	8.837E+11	8.656E+11	8.370E+11
12	7.00E-01 - 8.00E-01	1.216E+13	1.196E+13	1.142E+13	1.027E+13	9.101E+12	6.306E+12	5.471E+12	4.499E+12	3.566E+12	2.760E+12	1.172E+12
13	8.00E-01 - 9.00E-01	1.614E+12	1.580E+12	1.493E+12	1.343E+12	1.212E+12	8.240E+11	5.987E+11	2.017E+11	4.876E+10	1.820E+10	8.998E+09
14	9.00E-01 - 1.00E+00	1.183E+12	1.137E+12	1.026E+12	8.620E+11	7.486E+11	4.316E+11	2.617E+11	7.510E+10	2.052E+10	9.549E+09	5.733E+09
15	1.00E+00 - 1.10E+00	9.385E+11	8.748E+11	7.101E+11	4.169E+11	2.027E+11	2.234E+10	1.457E+10	9.401E+09	7.867E+09	7.167E+09	5.894E+09
16	1.10E+00 - 1.20E+00	6.870E+11	6.406E+11	5.263E+11	3.413E+11	2.197E+11	6.152E+10	2.342E+10	5.338E+09	4.521E+09	4.174E+09	3.458E+09
17	1.20E+00 - 1.30E+00	7.084E+11	6.588E+11	5.353E+11	3.334E+11	2.001E+11	4.770E+10	2.122E+10	7.835E+09	5.832E+09	4.668E+09	2.828E+09
18	1.30E+00 - 1.40E+00	3.946E+11	3.634E+11	2.999E+11	2.269E+11	1.817E+11	6.302E+10	2.297E+10	2.790E+09	2.144E+09	1.968E+09	1.631E+09
19	1.40E+00 - 1.50E+00	3.550E+11	3.304E+11	2.715E+11	1.832E+11	1.304E+11	5.240E+10	2.343E+10	7.840E+09	6.831E+09	6.308E+09	5.099E+09
20	1.50E+00 - 1.60E+00	2.853E+12	2.850E+12	2.842E+12	2.833E+12	2.822E+12	2.491E+12	1.942E+12	6.591E+11	1.299E+11	2.629E+10	1.090E+09
21	1.60E+00 - 1.70E+00	1.515E+11	1.369E+11	1.015E+11	4.713E+10	1.692E+10	1.781E+09	1.024E+09	6.990E+08	6.451E+08	6.024E+08	4.949E+08



22	1.70E+00 - 1.80E+00	2.227E+11	2.035E+11	1.566E+11	8.287E+10	3.890E+10	6.033E+09	2.359E+09	5.916E+08	5.322E+08	4.987E+08	4.115E+08
23	1.80E+00 - 1.90E+00	4.867E+10	4.223E+10	2.907E+10	1.483E+10	8.672E+09	2.110E+09	1.365E+09	6.409E+08	3.662E+08	2.956E+08	2.312E+08
24	1.90E+00 - 2.00E+00	9.214E+10	8.863E+10	7.951E+10	6.244E+10	4.783E+10	1.723E+10	6.406E+09	7.116E+08	4.492E+08	3.864E+08	3.076E+08
25	2.00E+00 - 2.10E+00	4.380E+10	4.072E+10	3.403E+10	2.531E+10	2.009E+10	8.088E+09	3.138E+09	4.398E+08	2.480E+08	2.015E+08	1.561E+08
26	2.10E+00 - 2.20E+00	4.379E+10	4.044E+10	3.364E+10	2.616E+10	2.261E+10	1.764E+10	1.606E+10	1.449E+10	1.336E+10	1.239E+10	9.949E+09
27	2.20E+00 - 2.30E+00	1.634E+10	1.482E+10	1.143E+10	6.933E+09	4.547E+09	1.538E+09	5.659E+08	5.240E+07	1.522E+07	7.214E+06	3.931E+06
28	2.30E+00 - 2.40E+00	5.878E+10	5.236E+10	4.030E+10	3.050E+10	2.849E+10	2.331E+10	1.750E+10	5.865E+09	1.277E+09	3.730E+08	1.298E+08
29	2.40E+00 - 2.50E+00	1.616E+10	1.455E+10	1.075E+10	5.126E+09	2.087E+09	6.022E+08	4.275E+08	2.161E+08	1.445E+08	1.241E+08	9.943E+07
30	2.50E+00 - 2.60E+00	1.029E+11	1.027E+11	1.024E+11	1.022E+11	1.020E+11	8.969E+10	6.978E+10	2.362E+10	4.626E+09	9.107E+08	1.201E+07
31	2.60E+00 - 2.70E+00	2.054E+09	1.605E+09	7.828E+08	1.439E+08	3.990E+07	1.316E+07	7.071E+06	4.031E+06	3.730E+06	3.484E+06	2.840E+06
32	2.70E+00 - 2.80E+00	7.598E+09	7.195E+09	6.165E+09	4.211E+09	2.442E+09	7.853E+07	3.101E+07	2.025E+07	1.895E+07	1.785E+07	1.491E+07
33	2.80E+00 - 2.90E+00	1.252E+09	1.201E+09	1.108E+09	1.030E+09	1.005E+09	8.747E+08	6.845E+08	2.404E+08	5.667E+07	2.014E+07	9.557E+06
34	2.90E+00 - 3.00E+00	1.170E+09	1.105E+09	1.005E+09	9.505E+08	9.423E+08	8.327E+08	6.498E+08	2.212E+08	4.434E+07	9.680E+06	1.128E+06

35	3.00E+00 - 4.00E+00	1.532E+09	1.333E+09	1.004E+09	7.799E+08	7.440E+08	6.546E+08	5.113E+08	1.753E+08	3.661E+07	9.348E+06	2.374E+06
36	4.00E+00 - 5.00E+00	1.998E+08	1.556E+08	7.494E+07	1.064E+07	5.853E+05	2.194E+02	1.070E+00	2.152E-01	2.151E-01	2.151E-01	2.151E-01
37	5.00E+00 - 6.00E+00	1.286E+06	6.827E+05	3.289E+05	4.659E+04	2.491E+03	6.176E-02	6.176E-02	6.175E-02	6.174E-02	6.174E-02	6.172E-02
38	6.00E+00 - 8.00E+00	3.350E+04	2.258E-02	2.258E-02	2.258E-02	2.258E-02	2.258E-02	2.258E-02	2.258E-02	2.257E-02	2.257E-02	2.256E-02
39	8.00E+00 - 1.00E+01	1.274E+01	2.092E-03	2.092E-03	2.092E-03	2.092E-03	2.092E-03	2.092E-03	2.092E-03	2.091E-03	2.091E-03	2.090E-03
totals		1.011E+14	9.859E+13	9.190E+13	7.904E+13	6.729E+13	3.975E+13	2.972E+13	1.767E+13	1.237E+13	9.906E+12	6.365E+12



Appendix A.2 39 SOSNY Specified Gamma Energy Groups (MeV)

83**	10.0+6	8.0+6	6.0+6	5.0+6	4.0+6	3.0+6	2.9+6	2.8+6	2.7+6	2.6+6	2.5+6	2.4+6	2.3+6	2.2+6	2.1+6
	2.0+6	1.9+6	1.8+6	1.7+6	1.6+6	1.5+6	1.4+6	1.3+6	1.2+6	1.1+6	1.0+6	0.9+6	0.8+6	0.7+6	0.6+6
	0.5+6	0.4+6	0.3+6	0.2+6	0.1+6	0.5+5	1.0+4	0.5+4	1.0+3	e					

Where **e** means to truncate

